Ion-Selective Electrodes With Ionophore-Doped Sensing Membranes

Philippe Bühlmann and Li D. Chen
University of Minnesota, Minneapolis, MN, USA

1 INTRODUCTION

At the time of this writing, more than 20 000 publications related to ion-selective electrodes (ISEs)[1–7] have been published, with approximately two new ones per day in recent years. Figure 1 shows, for the period between 1970 and 2009, the continuing increase in the number of publications that could be readily recognized as reporting on the preparation or use of ionophore-based ISEs. Clearly, this is still a fast growing field. Until the mid 1990s, most of the research in this field focused on the development of new ionophores that provided improved selectivities.[4] However, many leading analytical chemists who work in the field have since redirected their attention to an improved understanding of the thermodynamics and kinetics that describe the response and selectivity of ISEs, the development of new sensing modes and electrode designs, as well as the use of novel materials, such as novel polymer matrixes, nanostructured materials, or biomaterials. These efforts resulted in substantial progress, such as the lowering of detection limits from micro- to subpicomolar concentrations,[8–16] dramatic improvements of selectivities up to 10 and more orders of magnitude[16,17] from what used to be rarely more than five orders of magnitude, and major advancements in biocompatibility and long-term stabilities.[5,18–20] Unfortunately, there has been no major monograph summarizing the current state of the art of ISEs to an audience that is new to the field. Most recent reviews on ISEs are better suited for those who already have a substantial knowledge of ionophore-based ISEs and only wish to get an update on recent advances.

This chapter familiarizes the reader not only with the state of the art of ISEs, which was achieved by the application of sophisticated host–guest chemistry, but also with a modern view of the fundamentals of ionophore-based ISEs. It introduces the basic concepts of the thermodynamic ISE theory that has replaced, in recent years, the empirical approach taken in the early history of ISEs. This theory provides sophisticated tools to control sensor selectivities that are not immediately obvious given the concepts of host–guest chemistry in a homogeneous phase. A general knowledge of these tools will help the host–guest chemist to better identify needs and opportunities for the development of new ionophores, and it will introduce newcomers to the field of ISEs to fundamentals and important contributions from the original literature. The focus of the fundamental section of this chapter is not on details but on the understanding of major

Supramolecular Chemistry: From Molecules to Nanomaterials.
Edited by Philip A. Gale and Jonathan W. Steed.
ISBN: 978-0-470-74640-0.

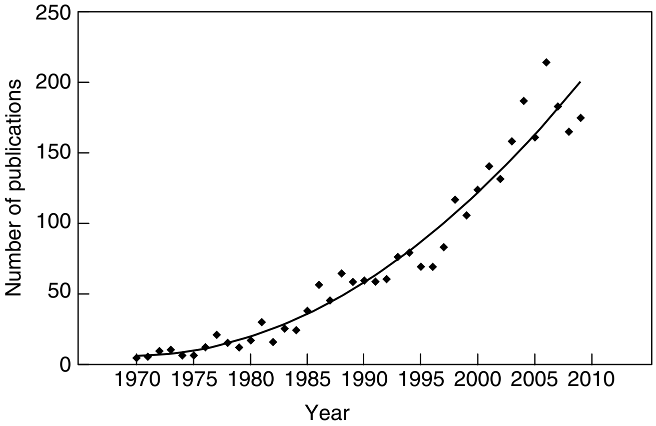

Figure 1 Number of publications that reported between 1970 and 2009 on the preparation or use of ion-selective electrodes (ISEs) with an ionophore-doped sensing membrane. Note that the numbers shown are conservative estimates that are likely too low because they only include publications that explicitly refer to an ionophore or carrier.

concepts and the elimination of misconceptions. Only a minimum number of equations are used, and the interested reader is referred to the original literature and more specialized reviews for further reading. For the sake of simplicity, certain details such as reduced activity coefficients at higher concentrations, ion pairing effects, and liquid junction potentials within sandwich membranes have been omitted here. We believe that such effects go beyond the scope of this chapter and that the interested reader will certainly find them discussed appropriately in the original literature.

Importantly, this chapter shows not only how modern potentiometry allows the extremely efficient application of ionophores but also illustrates how ionophore-based potentiometry can be used to determine thermodynamic properties of ionophores such as the stoichiometries and stabilities of their complexes with a wide range of ions. Indeed, it is still often overlooked that ion-selective potentiometry with ionophore-doped sensing membranes not only benefits from ionophores developed by host–guest chemists, but that it also provides sophisticated methods to characterize the ion-binding properties of ionophores, polymers, and other compounds. As several thousand research articles show, those who practice molecular recognition have been using pH-selective glass electrodes for more than half a century to monitor host–guest complexation in the aqueous phase.[21,22] However, many researchers practicing outside of the ISE field have yet to recognize that potentiometry is also extremely useful to study the host–guest chemistry of ionophores in the microliter volume of hydrophobic ISE membranes, using in a very economic fashion only a few milligrams of ionophore. Therefore, the goal of this chapter is not only to give a brief history of ISEs (Section 2), show how host–guest chemistry is used to design ionophores (Section 4), and use them efficiently in ISEs (Section 3) but also to illustrate how ionophore-based ion-selective potentiometry can be used by host–guest chemists as a tool to investigate host–guest chemistry (Section 5).

2 ION-SELECTIVE POTENTIOMETRY MEETS HOST–GUEST CHEMISTRY

The senses are key to life as they permit the perception of outside stimuli. The commonly cited ones include hearing, touch, sight, taste, and smell, and allow humans to obtain physical and chemical information about their environment. Attempts to use the same principles and build instrumentation that measures such parameters have resulted in sensors that measure physical parameters, such as pressure, temperature, and the intensity of light, as well as chemical sensors that can be used to measure the concentration of specific chemical species in air and water. Arguably one of the most successful types of chemical sensors are ISEs, which can be used to determine the concentration of selected ions by comparatively simple measurements of electrical potentials with a voltmeter (Figure 2).

The history of ISEs goes back all the way to 1906, when Max Cremer discovered pH-sensitive glasses,[23] which led to the first commercial pH glass electrodes in the 1930s.[24] The introduction of crystalline compounds such as LaF_3, AgCl, or Ag_2S as sensing materials in the early 1960s considerably expanded the number of ions that could be measured. Among the most notable ISEs of this type are the fluoride- and halide-selective electrodes.[1] While ISEs based on glasses and the crystalline materials are extremely useful for many applications, the further development of ISEs based on these materials was hindered by the difficulty of designing crystalline materials with selectivities for particular ions of interest. Fine tuning of the glass composition led to the discovery of materials responding to other ions, such as Li^+ and Na^+, but the selectivities of sensors based on these glasses remained restricted.[4] Moreover, the use of crystalline compounds as sensing materials is limited by the poor ionic conductivity of most crystalline compounds. However, at a point in time when the further development of ISEs stalled and it appeared that these sensors were going to be suitable for the analysis of only a limited number of chemical species of interest, ISEs based on ion-binding receptors (i.e., ionophores or ion carriers) were introduced. This completely transformed the field of ISEs, and was the onset of a long-lasting impact of host–guest chemistry on the development of chemical sensors.

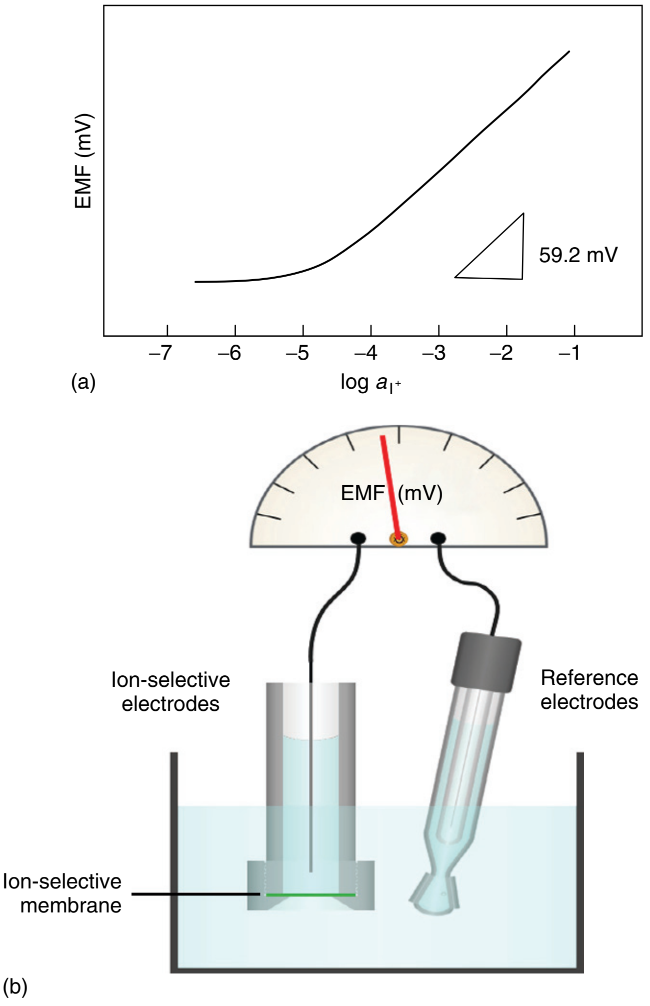

Figure 2 (a) Potentiometric response and (b) experimental setup in a conventional ion-selective electrode measurement.

The earliest work with ISEs based on electrically neutral ionophores was inspired by the observation of Moore and Pressman that the antibiotic valinomycin (Figure 3), **K^+-I**, caused the uptake of K^+ into and the release of H^+ from mitochondria.[25] Simon and Stefanac showed in 1966 that thin films of water-immiscible organic solvents doped with antibiotics exhibited responses to monovalent cations with selectivities similar to those observed in biological systems.[3,26,27] While the very first examples of such ISEs used the ammonium-selective receptors nonactin (**NH_4^+-I**) and monactin (**NH_4^+-II**), the ISE based on the antibiotic valinomycin reported shortly afterwards[28] has become one of the best known ISEs. The fame of the valinomycin-based ISE stems from its high K^+ selectivity, which permits K^+ measurements in biological samples, such as blood, and has made this ISE a commercial success to this day.

The 1960s were also a period in which the field of host–guest chemistry made tremendous advances, as exemplified by the Nobel prize-winning development of crown ethers. Not surprisingly, both analytical and organic chemists quickly set out to develop synthetic ionophores for use in ISEs. The result of this development was that ion-selective potentiometry replaced flame atomic emission spectroscopy in the 1980s as the standard technique for the measurement of electrolyte ions in blood and urine. Well over a billion measurements are performed annually with ISEs, making this type of sensor one of the biggest successes of host–guest chemistry.[4,29,30] This is also reflected by the many subject areas in which articles on ISEs have been published, which include not only analytical chemistry but also other fields of chemistry, environmental sciences, medicine, engineering,

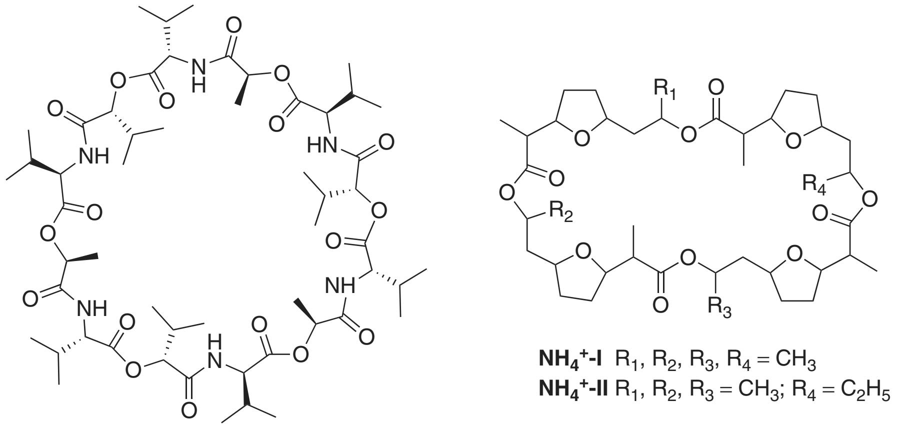

NH_4^+-I $R_1, R_2, R_3, R_4 = CH_3$
NH_4^+-II $R_1, R_2, R_3 = CH_3$; $R_4 = C_2H_5$

K^+-I

Figure 3 Structures of the three antibiotics valinomycin, nonactin, and monactin, which continue to be widely used as ionophores for ISE membranes.

pharmacology, biochemistry, food science and technology, physiology, neurosciences, and agronomy, to name just a few.

The original development of ionophore-based ISEs, with an experimental setup strongly resembling the glass electrode, was followed by the introduction of several related techniques. Among the earliest ones were microelectrodes (Section 3.1.6),[31–33] ISEs with integrated enzyme layers, and ISEs modified with gas-permeable membranes for the detection of electrically neutral, volatile species such as ammonia and carbon dioxide (Section 3.1.7).[34] The experimental limitations associated with the inner filling solution separating the ion-selective membrane from the inner reference element inspired several proposals for so-called solid-contact ISEs (Section 3.1.5).[35–38] Eventually, even the dogma of using these ionophore-doped ion-selective membranes in a potentiometric mode, that is, in the absence of net ionic current, was swept away when ionophores started to be used in ion-transfer voltammetric,[39,40] galvanostatic,[41,42] and coulometric methods (Section 3.1.8).[43,44] Notwithstanding, the general concepts of ionophore-based potentiometry, as they are discussed in Sections 3 and 5, are common to all these techniques.

3 A PRIMER TO IONOPHORE-BASED POTENTIOMETRY

3.1 The origin of the potentiometric response

3.1.1 Phase boundary potentials

Above their detection limit, ISEs respond to ions with changes in the measured electrical potential, as illustrated in Figure 2. For historical reasons, the measured potential is typically referred to as electromotive force, EMF. At room temperature, a 10-fold increase in the activity of the ion i with the charge z_i results in an increase in the EMF of 59.2 mV/z_i, as predicted for 25 °C by the Nernst equation[3,45]:

$$\mathrm{EMF} = E^\circ + \frac{RT}{z_i F}\ln a_i = E^\circ + \frac{2.303RT}{z_i F}\log a_i \qquad (1)$$

The term E° is a constant, as will be discussed with more detail below. The origin of this EMF response is directly related to the sample dependence of the electrical potential difference across the phase boundary between the sample phase and the hydrophobic ion-selective phase. Therefore, before considering any other experimental aspects, let us have a closer look at the phase boundary between ionophore-doped hydrophobic phases and aqueous samples. While Section 3.1.3 will briefly comment on the role of the reference electrode and the inner reference element of an ISE, the following discussion emphasizes that the phase boundary between the sample phase and the hydrophobic ion-selective phase is what needs to be considered to understand why an ISE responds to the ion of interest, and how the selectivities of ISEs for the target over other ions can be explained quantitatively.

Phase boundary potentials are much more common than the nonelectrochemist may suspect, and are quite easy to understand intuitively. Consider for example, an organic chemist who is interested in phase transfer catalysis and uses an extraction funnel filled with equal volumes of water and a water-immiscible organic solvent (Figure 4). Upon addition of tetrabutylammonium nitrate and complete equilibration of the two phases, there will be tetrabutylammonium nitrate in both phases. Because of the requirement for electroneutrality in bulk phases, the concentration of tetrabutylammonium ions (shown in Figure 4 as C^+) in the aqueous phase will equal the concentration of nitrate ions (A^-) in the aqueous phase. While the concentration of tetrabutylammonium ions in the organic phase will differ from that in the aqueous phase because of the different energies of tetrabutylammonium nitrate solvation in the aqueous and organic phase, the tetrabutylammonium ion concentration in the organic phase will again (because of bulk electroneutrality) equal the concentration of the nitrate ions in the bulk of the organic phase. Only in very close proximity of the phase boundary between the aqueous and organic phase, the different characters of the two types of ions will manifest themselves as an imbalance between the local concentrations of cations and anions. For example, in the case of 1,2-dichloroethane as the organic phase, the nitrate ion prefers the aqueous phase. Indeed, the transfer of nitrate ions from 1,2-dichloroethane into the aqueous phase is favored by 33.9 kJ mol^{-1}.[46] On the other hand, the hydrophobic tetrabutylammonium ion prefers the organic phase, as shown by the Gibbs energy of partition between water and 1,2-dichloroethane of −21.8 kJ.[46] The different affinities of the two ions for the two phases result in charge separation across the interface between the aqueous and organic phases. While there will be a small excess of negative nitrate ions on the aqueous side of the interface, there will be a small excess of positive tetrabutylammonium ions on the organic side of the interface. This interfacial charge separation is the origin of the interfacial phase boundary potential. In Figure 4, the thin interfacial region in which charge separation occurs is schematically shown as the region between the two dashed red lines. In full consistency with electroneutrality, the excess of positive ions on one side of the phase boundary equals the excess of negative ions on the other side of the phase boundary.

A considerable amount of research has been performed to investigate the structure of such interfaces at the molecular

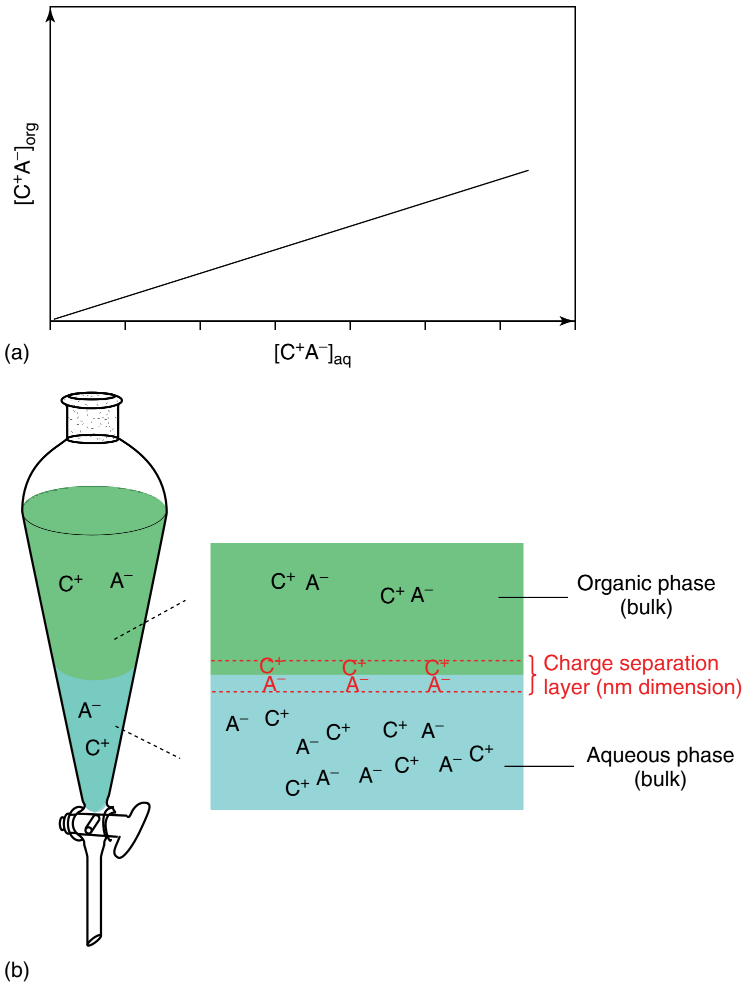

Figure 4 Equilibrium distribution of a single salt with the cations C^+ and anions A^- between an aqueous and a water-immiscible organic phase: The ratio of the salt concentrations in the two phases is given by the distribution coefficient. Charge separation occurs across the phase boundary but there is electroneutrality in both bulk phases.

level, for example, in order to determine how sharp the transition from water to the organic solvent is and how ions distribute spatially within the charge separation layer.[47] Not surprisingly, there are differences for different solvents and ions, and the concentrations of the involved salts play an important role too. In order to understand the response mechanism of an ionophore-based ISE, such details are luckily irrelevant. The only important information for an intuitive understanding of phase boundary potentials is that the thickness of the charge separation layer within which electroneutrality can be violated is only on the order of nanometers.[47]

The above description of the phase boundary between an aqueous and an organic salt solution readily permits an intuitively easily understandable conclusion: the phase boundary potential depends on the type of ions involved. Consider, for example, the interface between an aqueous and an organic phase both containing tetrabutylammonium nitrate, and compare it to the interface between an aqueous and an organic phase containing the nitrate salt of tetrapropylammonium, which has a total of four methylene groups less. The phase boundary potential at the former interface will be larger than at latter interface since the preference of the tetrapropylammonium ion for the organic phase is smaller than it is in the case of the tetrabutylammonium ion. For the case of the organic solvent 1,2-dichloroethane, for example, the Gibbs free energy of partition of the tetrapropylammonium ion is only $-8.8\,\mathrm{kJ\,mol^{-1}}$, which is much smaller than the value of $-21.8\,\mathrm{kJ\,mol^{-1}}$ for the tetrabutylammonium ion.[46]

A somewhat less intuitive fact is that the phase boundary potential at the interface between two phases that contain only one salt (the so-called distribution potential) does not depend on concentration of this salt (unless its concentration is so high that activity coefficients differ substantially from unity).[48] On a qualitative level, this may be understood by the fact that any concentration-induced increased tendency of the nitrate to transfer from the organic into the aqueous phase is countered by an equivalent concentration-induced increase in the tendency for the tetraalkylammonium ion to follow nitrate into the aqueous phase, and vice versa. From the view of thermodynamics, the concentration independence of the phase boundary potential in this particular case can be explained quantitatively with a very general equation that describes the phase boundary potential, E_{PB}, at equilibrium:

$$E_{\mathrm{PB}} = E^{\circ}_{\mathrm{PB},i} + \frac{RT}{z_i F} \ln \frac{a_{i,\mathrm{water}}}{a_{i,\mathrm{organic}}} \tag{2}$$

where $E^{\circ}_{\mathrm{PB},i}$ is a constant that depends on the solvation energies of the ion i in the two phases. The derivation of this equation from electrochemical potentials is straightforward, as shown in the literature.[3,45,49] Clearly, as long as the addition of more salt into the two-phase system raises the activities of the ion i in both phases by the same factor, the phase boundary potential, E_{PB}, does not depend on the salt concentration.

In the case of one or multiple salts distributing between two immiscible liquids, $E^{\circ}_{\mathrm{PB},i}$ is different for every ion involved since this value depends on ionic solvation. However, since there is only one physical phase boundary, there is also only one value for the phase boundary potential, E_{PB}, between the two phases. In the example of the single salt distributing between the two phases, the same value of E_{PB} is obtained when (2) is applied to the cation as when it is applied to the anion, which can be understand upon realizing that the charge z_i of the two ions differ.

3.1.2 *Essential components of an ionophore-doped ISE membrane: ionophore and ionic sites*

Equation (2) for the phase boundary potential applies not only to distribution potentials but can be used for any number of ions that are distributed between two immiscible solutions. Most importantly, it applies to the sample–membrane interface of any type of ISE. Indeed, one of the most fundamental principles of ISEs can be directly obtained by rearrangement of (2). If the activity of the ion of interest in the bulk of the water-immiscible sensing phase is constant and does not depend on the sample, the phase boundary potential at the interface of the sample and an ionophore-doped hydrophobic phase has the same dependence on the ion activity as the desirable Nernstian response of an ISE (1)[50]:

$$\begin{aligned} E_{\mathrm{PB}} &= E^{\circ}_{\mathrm{PB},i} + \frac{RT}{z_i F} \ln a_{i,\mathrm{water}} + \frac{RT}{z_i F} \ln \frac{1}{a_{i,\mathrm{organic}}} \\ &= E^{\circ\prime}_{\mathrm{PB},i} + \frac{RT}{z_i F} \ln a_{i,\mathrm{water}} \end{aligned} \tag{3}$$

The two key tasks for the scientist who fabricates and uses an ISE are (1) to assure that the activity of the ion of interest in the bulk of the water-immiscible sensing phase is constant and does not depend on the sample composition, and (2) to ensure that, except for E_{PB}, all contributions to the measured EMF are sample independent (for the latter, see Section 3.1.2). If these two requirements are fulfilled, an ISE will respond to the ion of interest with the desired Nernstian response.

To illustrate which components are necessary to prepare an ISE membrane, let us again go back to a simple extraction experiment as it was similarly described in Section 3.1.1. Consider an aqueous potassium chloride solution equilibrated with an immiscible organic phase containing an electrically neutral ionophore for K^+, that is, a receptor compound that binds the potassium ion selectively. How does the phase boundary potential between these two phases depend on the KCl concentration in the aqueous phase? Upon equilibration of the two phases, some KCl will be present in the organic phase (Figure 5). For low amounts of KCl in the system, the potassium ions in the organic phase will be present in the form of ionophore complexes, and there will be an excess of free ionophore, L. In comparison to the concentration of the ionophore complex, the organic phase concentration $[K^+]$ of free potassium ions that are not bound by the ionophore is very low and can be calculated from the formation constant, $\beta_{1:1}$, of the potassium ion complex, $[LK^+]$:

$$\beta_{1:1} = \frac{[LK^+]}{[L][K^+]} \Longrightarrow [K^+] = \frac{[LK^+]}{[L]\beta_{1:1}} \tag{4}$$

The higher the KCl concentration in the aqueous phase is, the higher the complex concentration and the lower the concentration of free ionophore in the organic phase becomes. Consequently, the ratio of free and complexed ionophore changes and, as shown by (4), the free potassium concentration in the organic phase depends on the activity of the potassium ions in the aqueous phase. Indeed, for an excess of ionophore, the concentration of free potassium ions in the organic phase is directly proportional to the activity of the potassium ions in the aqueous phase, and it follows from (2) that in this range the phase boundary potential does *not* depend on the potassium ion concentration in the aqueous phase. The E_{PB} obtained under these circumstances is again a distribution potential (Section 3.1.1) independent of the salt concentration in the aqueous phase. However, this phase boundary potential differs from the one in the absence of ionophore because the excess ionophore facilitates the phase transfer of the potassium ion into the organic phase and, therefore, considerably increases the total concentration of KCl in the organic phase. Importantly, because of the independence

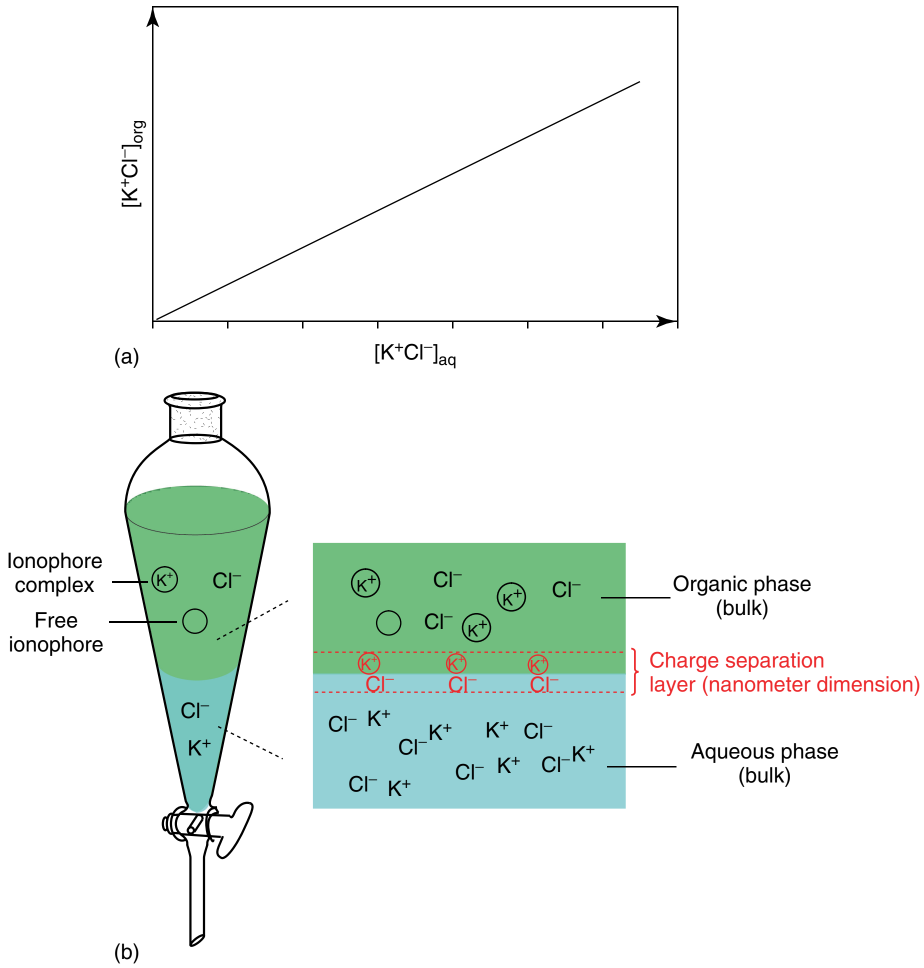

Figure 5 Equilibrium distribution of KCl between an aqueous phase and a water-immiscible organic phase that contains a K^+-binding ionophore. The ionophore increases the solubility of the salt in the organic phase.

of this phase boundary potential on the K^+ concentration in the aqueous phase, it cannot be the basis of the sample dependent EMF of an ISE. Simply doping a water-immiscible organic thin film with ionophore does not make an ion-selective membrane suitable for potentiometry.[51]

The trick necessary to keep the activity of the ion of interest in the bulk of the water-immiscible sensing phase sample-independent is to add to the organic phase in addition to the electrically neutral ionophore also a hydrophobic ion that has a charge sign opposite to the charge sign of the measured ion (Figure 6). In the example of a K^+ ionophore, such an ion could be, for example, a tetraphenylborate derivative (Figure 7). Owing to the requirement of electroneutrality, the total concentration of (free and complexed) potassium ions in the bulk of the organic phase equals the concentration of all anions in this phase. As long as the hydrophobic anion is the only anion present in the organic phase at a substantial concentration, the K^+ concentration in the organic phase does not depend on the KCl concentration in the aqueous phase, and it follows from (3) that E_{PB} shows a Nernstian dependence on the potassium ion activity in the aqueous sample.[52]

Importantly, the hydrophobic anion suppresses the extraction of chloride into the organic phase, as can be seen from the equilibrium constant K_{ex} that governs the distribution of KCl between the two phases.

$$K^+_{aq} + Cl^-_{aq} \rightleftharpoons K^+_{mem} + Cl^-_{mem} \tag{5a}$$

$$K_{ex} = \frac{a_{K^+,\,mem}\, a_{Cl^-,\,mem}}{a_{K^+,\,aq}\, a_{Cl^-,\,aq}} \tag{5b}$$

In the absence of a hydrophobic anion in the organic phase, the concentrations of K^+ and Cl^- in the organic phase are equal. However, when the concentration of K^+ in the organic phase is very high because these ions balance the negative charge of the hydrophobic counteranions (R^-), the consequence of (5b) is that $a_{Cl^-,\,mem}$ becomes very low. This can be considered to be a Le Chatelier effect on the KCl distribution between the two phases (5a); a high

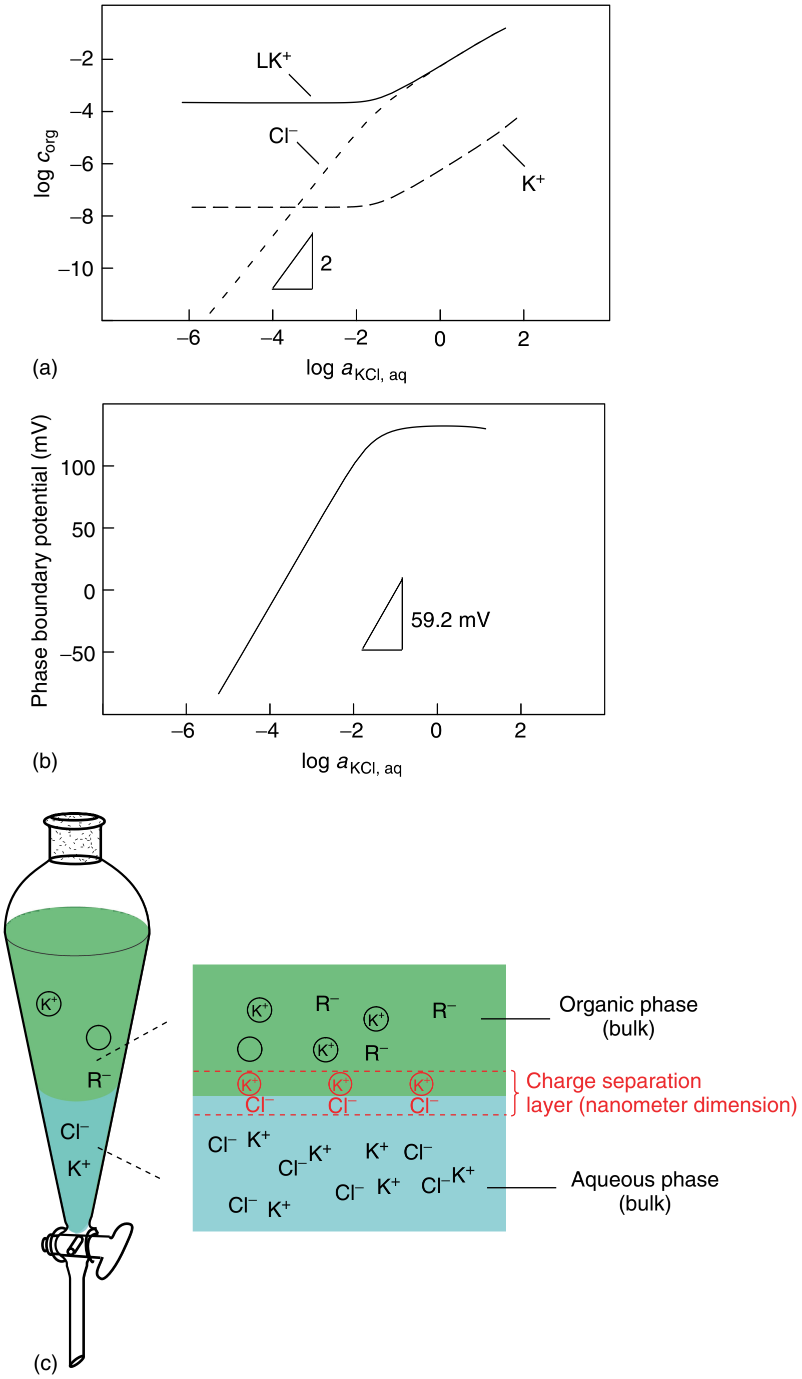

Figure 6 Equilibrium ion distribution between an aqueous KCl solution and a water-immiscible sensing phase doped with a K^+ ionophore (L) and anionic sites (R^-): The phase boundary potential at the interface of the aqueous and organic phase is the origin of the familiar Nernstian response of ISEs. Note that within the Nernstian response range the Cl^- concentration in the organic phase is extremely small, and the vast majority of K^+ in the membrane is in the complexed form.

concentration of K^+ in the organic phase favors chloride transfer into the aqueous phase.

In the older potentiometric literature hydrophobic ions used as counterions to the analyte ion have been sometimes referred to as ion excluders. In the current literature, they are typically referred to as ionic sites. It follows from the discussion above that ionic sites are a necessity for the proper functioning of ISEs based on *electrically neutral* ionophores.[51] Ionic sites are not required to ensure that ISE membranes doped with *electrically charged* ionophores exhibit a Nernstian response to the ion of interest, but as it is also true for the electrically neutral ionophores, ionic sites

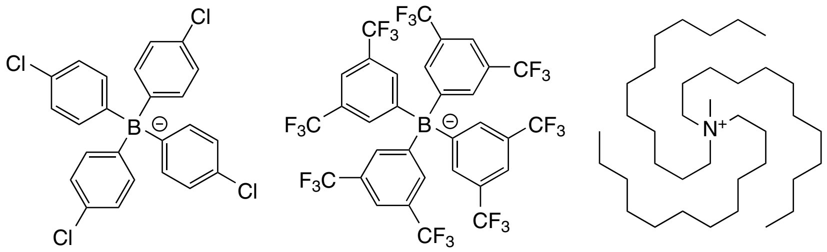

Figure 7 Common highly hydrophobic ionic sites used to dope ISE membranes.

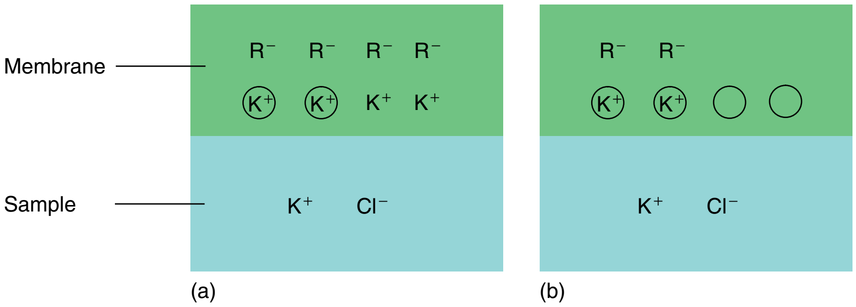

Figure 8 Equilibrium ion distribution between an aqueous KCl solution and an ISE membrane with a ratio of K^+ ionophore and cationic sites of (a) 1 : 2, and (b) 2 : 1.

used in an optimized ratio to the ionophore can improve the selectivity (Section 5.2).[53]

Note that the concentration of ionic sites has to be low enough so that the organic phase contains a substantial concentration of free ionophore. For example, consider an organic phase prepared to contain an anionic site and an electrically neutral ionophore that binds K^+ with 1 : 1 stoichiometry. If the molar ratio of ionic sites and ionophore is 2 : 1 and the organic phase is equilibrated with an aqueous KCl solution, all of the ionophore will be present in the form of K^+ complexes, and only half of the K^+ ions will be able to bind to an ionophore (Figure 8a). Because of the very substantial concentration of uncomplexed K^+ in the organic phase, the phase boundary potential will be identical to the one observed for an ionophore-free organic phase containing only ionic sites. On the other hand, if the molar ratio of ionic sites and ionophore is 1 : 2 and the organic phase is equilibrated with an aqueous KCl solution, half of the ionophore will be present in the form of K^+ complexes, half of the ionophore is in its uncomplexed form (Figure 8b), and the phase boundary potential exhibits the selectivity characteristic for an ionophore-doped organic phase. This latter situation is similar to the one of pH buffers, which only exhibit good buffering capacities if they contain substantial concentrations of both an unprotonated base and the conjugated acid (i.e., the proton complex of the conjugated base). Following this analogy, we can simplify the above statement that "a Nernstian ISE response requires that the activity of the ion of interest in the bulk of the water-immiscible sensing phase is constant and does not depend on the sample." More succinctly, a Nernstian ISE response requires that the ionophore and the ionic sites buffer the ion of interest in the sensing phase.

3.1.3 The conventional ISE measurement

As shown above, the phase boundary potential at the interface between an aqueous sample and the hydrophobic sensing phase of an ISE membrane depends logarithmically on the activity of the ion of interest in the aqueous sample (3). However, an experimental method to measure this phase boundary potential directly does not exist. The reason why potentiometric measurements, nevertheless, exhibit the same logarithmic dependence on the activity of the ion of interest in the sample is illustrated in Figure 9. The actual potentiometric measurement determines the EMF as the difference in the electrical potentials between the connecting wire of the ISE and the connecting wire of a reference electrode. As in every electrochemical cell, the EMF is the sum of two types of components: One type of contributions to the measured EMF arises from the phase boundary potentials at all interfaces of the electrochemical cell. Figure 9 illustrates the various phase boundary potentials present along the path from the copper connector of a typical ISE through the selective electrode, the sample, and the reference electrode. These phase boundary potentials include interfaces of different types, such as metal–metal, metal–salt, salt–liquid, and liquid–liquid interfaces. The other types of components that contribute to the measured EMF of an electrochemical

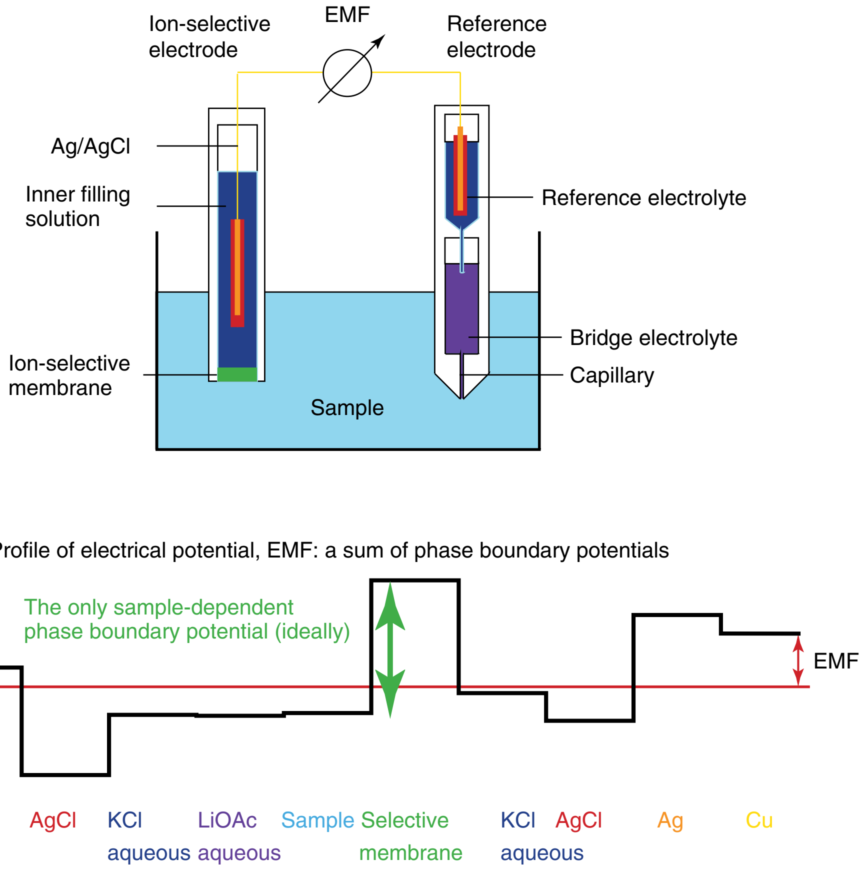

Figure 9 In the ideally currentless potentiometric measurement with an ISE, the measured potential is the sum of the all phase boundary potentials.

cell are associated with ohmic drop, V_{ohm}. The latter is the potential difference between the two ends of any ionic or electric conductor with resistance R when an electrical current, i, flows through it. It can be readily calculated as Ri, but since ion-selective potentiometry is almost always performed under nearly perfectly currentless conditions, the ohmic drop in an ISE measurement is negligibly small. Consequently, the EMF in a potentiometric measurement equals the sum of all phase boundary potentials, as they are illustrated in Figure 9.

Importantly, only two phase boundary potentials arise at interfaces between the sample and a neighboring phase and, consequently, all but those two phase boundary potentials add up to one sample-independent term, E_{const}:

$$\begin{aligned}\mathrm{EMF} &= \sum E_{\mathrm{PB}}\\ &= E_{\mathrm{const}} + E_{\mathrm{PB(salt\ bridge/sample)}} + E_{\mathrm{PB(sample/ISE\ membrane)}}\\ &\approx E'_{\mathrm{const}} + E_{\mathrm{PB(sample/ISE\ membrane)}} \qquad (6)\end{aligned}$$

Indeed, by choosing an appropriate electrolyte of high concentration for the salt bridge separating the sample from the reference electrode (lithium acetate in the example of Figure 9), the phase boundary potential at the salt bridge/sample interface can be kept very small and sample independent.[1,54] The only remaining phase boundary potential that is not included in the constant term is the phase boundary potential between the aqueous sample and the ionophore-doped sensing phase, which explains the logarithmic dependence of the EMF on the sample activity.

In the classical ISE setup, the ionophore-doped hydrophobic sensing phase separates the sample from the inner filling solution of the selective electrode. It is typically referred to as ion-selective membrane, a term that should, however, be interpreted with care. In most other applications of membranes, such as in filtration, osmosis, electrolysis, and gas separation, selective transport through the membrane is a key requirement and high transmembrane fluxes are very desirable. The complete opposite is true for ISE membranes. While ion movements over nanometers within the charge separation layer at the phase boundary between the sample and the membrane phase are key to the establishment of the ISE response, net ion transport through ISE membranes is not a requirement for the ISE response. Quite to the contrary, net fluxes of the ions of interest between the sample and the inner filling solution of an ISE worsen

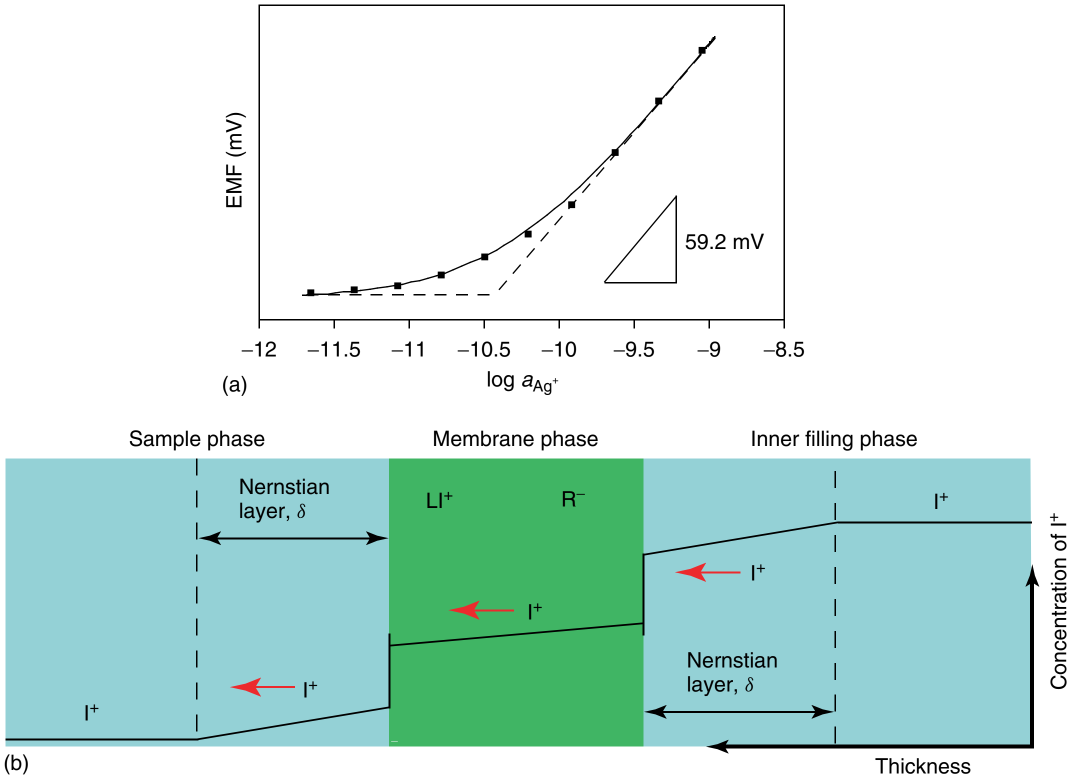

Figure 10 (a) Parts per trillion (ppt) detection limit for Ag^+ achieved by suppression of net ion fluxes. (Reproduced from Ref. 16. © ACS, 2010.) (b) Schematic illustration of how the flux of the target ion I^+ from the inner filling solution of an ISE through the sensing membrane into the sample can contaminate samples, worsening potentiometric detection limits.

detection limits (Figure 10). Indeed, the discovery of this phenomenon and the subsequent development of techniques to suppress such ion fluxes in the late 1990s allowed to lower the detection limits of ionophore-based ISEs from the micromolar to nano- and picomolar range.[8–16] The detection limit is also the only key performance characteristic for which the thickness of the ISE membrane is relevant. While the membrane thickness has no direct effect on the selectivity and response time of an ISE, thinner membranes increase the (typically extremely low) transmembrane ion fluxes and worsen detection limits.

Because potentiometric responses only require ion movements over nanometers at the phase boundary of the sample and the ion-selective membrane, ISEs have inherently very fast response times. With special equipment that permitted extremely fast sample exchange, response times of the order of microseconds have been demonstrated.[55] Response times of several seconds as they are often observed in routine measurements should not be misinterpreted as inherent characteristics of the electrode membrane. They are typically not related to properties of the ISE membrane itself but rather to how quickly the unstirrable layer of sample adhering to the ISE membrane can be exchanged for a new sample.

Because ISE responses do not depend on any type of ion current or flux, they are much less affected by adsorption of contaminants onto the sensor membrane than most other electrochemical and optical sensors. As long as adsorbed contaminants do not completely cover the ISE membrane, they have no effect on the measured response. However, in contrast to sensors based on solid sensing phases, such as metals in voltammetric sensors or inorganic salts in solid-state ISEs, extraction of hydrophobic sample components into the hydrophobic sensing membranes of ionophore-doped ISEs can result in the deterioration of the ISE selectivity.[56] This is of particular concern in the case of long-term measurements in biological samples.

3.1.4 Polymeric phases as inert matrixes for the ion-selective membrane

In the above examples, the ionophore-doped ion-selective membranes have been referred to as a hydrophobic phases. Historically, the earliest examples of such membranes were prepared as ionophore solutions in an organic water-immiscible solvent infused into some type of porous support, such as a porous glass filter. In 1970, polymeric membrane matrixes were introduced to improve the

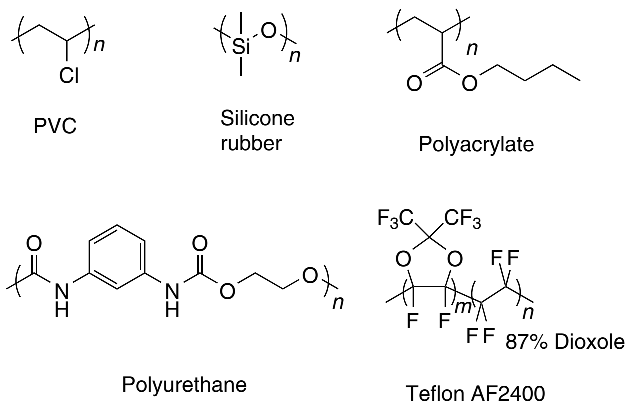

Figure 11 Polymer matrixes used to prepare ion-selective electrode membranes.

mechanical stability, and in particular, resistance to external pressure, of such devices.[57] While poly(vinyl chloride) (PVC) continues to be the most common matrix polymer for ISE membranes,[58,59] many other polymers have been successfully used (Figure 11). They include silicone rubbers, polyurethanes, acrylates, perfluoropolymers, and many others.[3] It is important that in all these cases, the polymers do not form any type of channels or have any other three-dimensional architecture. Instead, the ideal polymer provides a rubberlike homogenous hydrophobic medium in which the ionophore, ionophore complexes, and ionic sites can move freely, as they can do it in a water-immiscible organic solvent. However, to be able to function properly as an ISE membrane matrix, a polymer must fulfill a number of requirements, which will be briefly explained in the following paragraphs.

Because the sample-dependent phase boundary potential can only establish if the ions of interest can move freely back and forth between the aqueous sample and the membrane phase, crystalline polymers and amorphous polymers that form hard and brittle glasses at room temperature are not suitable as ISE membrane matrixes. Many successful polymers are soft and rubberlike amorphous materials that only transform into a glassy state well below room temperature. Others, such as poly(vinyl chloride) or Teflon AF, have a glass transition temperature that is high, but can be lowered below room temperature by blending with plasticizers.[60–62] The latter are liquids that are fully miscible with the polymer, have much lower molecular weights than the polymer itself, but have sufficiently low vapor pressures so that evaporation during the use of the ISE is not a concern (Figure 12). Plasticizers are not only components of many ISE membranes, but are used in many polymeric consumer products.

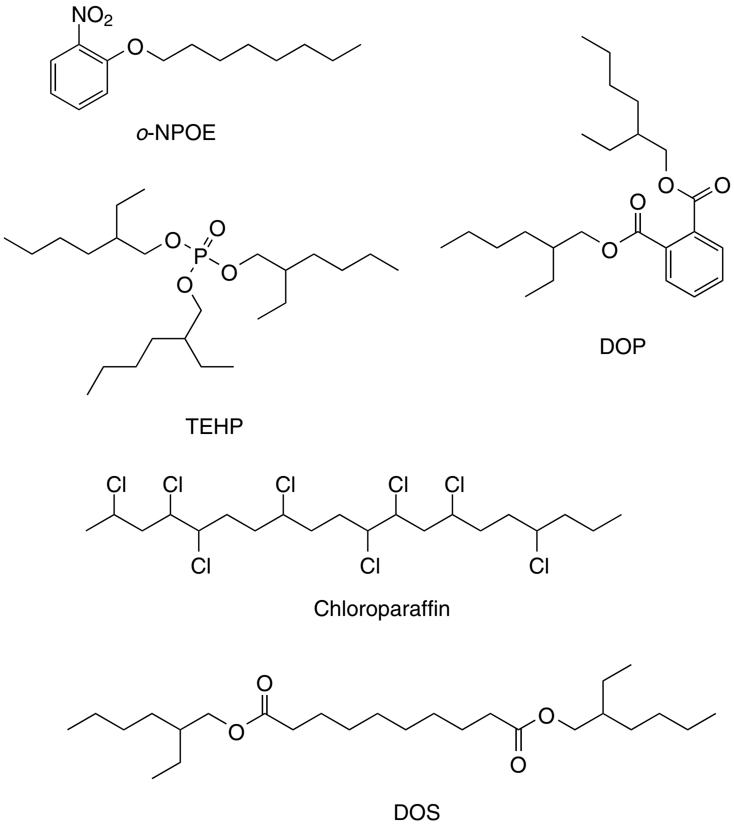

Figure 12 Plasticizers used for the preparation of ISE membranes.

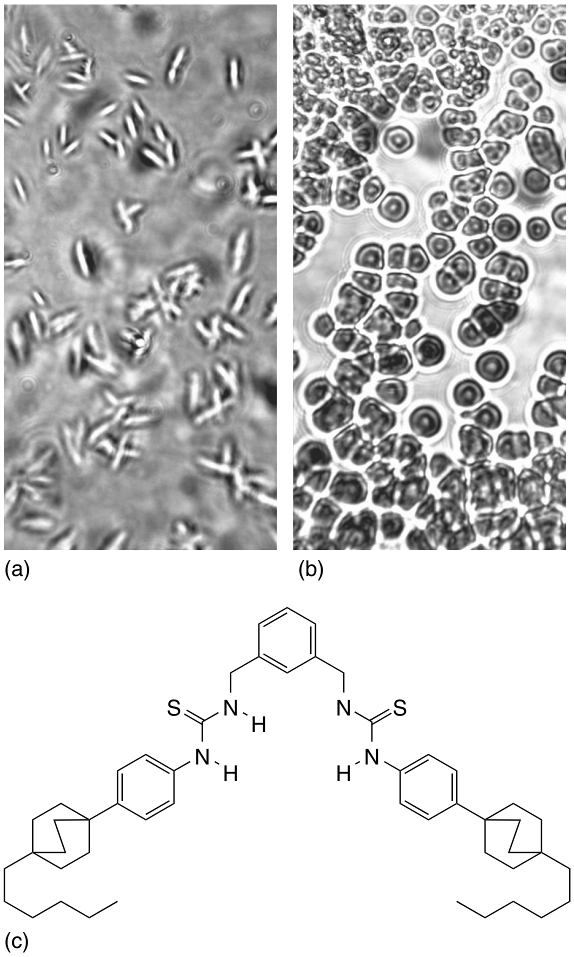

Figure 13 Ionophore aggregation in ISE membranes: Dark field microscopy images of membranes containing a bis-thiourea ionophore (c) and 0 or 50 mol% cationic sites (a and b, respectively) after exposure of the membranes to aqueous sulfate solutions. (Reproduced from Ref. 63. © Wiley-VCH, 2005.)

The matrix formed by the polymer or the blend of polymer and plasticizer must dissolve all the components that provide the ISE membrane with selectivity, that is, the free ionophore, the ionophore complex, and the ionic sites. In the case of an electrically neutral ionophore, this means that precipitation of not only the ionophore itself but also salts formed by the ionic sites and the ionophore complex must be avoided. In the laboratory, the formation of crystalline precipitates is often readily recognized with the naked eye. Because the aggregation of membrane components can also result in small crystals or noncrystalline aggregates that may be easily overlooked, the routine observation of ISE membranes containing new ionophores or ionic sites with an optical microscopy is recommended (Figure 13).[63] When a new ionophore or ionic site has been synthesized but is found to be affected by solubility problems, a very simple approach to deal with this problem is to choose a different polymeric matrix with which precipitation can be avoided. This is often also accompanied by typically minor but sometimes larger changes in selectivity.[1,3] If a different polymer or a different blend of polymer and plasticizer that dissolves the ion-selective components better cannot be found, the more cumbersome approach of synthesizing a more soluble compound has often to be taken. This may involve the attachment of unbranched or branched alkyl substituents to the ionophore or ionic site, or the reduction of compound symmetry. Alternatively, the ion-selective components may be covalently attached to the polymer backbone.[64]

To form a hydrophobic membrane suitable for use in potentiometry, a polymer cannot have that many polar groups that it becomes soluble in water. Even for a polymer of negligible solubility in water, polar substituents can be a disadvantage, though. In an ideal ISE membrane, the ion of interest is bound selectively by the ionophore, and any other type of ion undergoes only minimal stabilizing interactions with the membrane components. Evidently, after spending a lot of effort to design ionophores that strongly bind the ion of interest and form no or only very weak complexes with other ions, it is not desirable if other (potentially interfering) ions bind to the polymer or plasticizer, lowering the selectivity of the ISE membrane.[62] From this point of view, membrane matrixes of low polarity are desirable. The ultimate limit of selectivity may arguably be reached with fluorous matrixes, which are the least polar of all known condensed phases. Indeed, fluorous membrane ISEs have shown exceptional selectivities.[16,65–67]

3.1.5 ISEs with internal solid contacts

The conventional ISE setup with an inner filling solution separating the ion-selective membrane from an internal reference such as a AgCl-coated silver wire is very versatile and can be easily set up in the laboratory, it but brings along a number of disadvantages. These include insufficient resistance toward high pressure as encountered in sterilization and deep-sea measurements, and frailty of miniaturized sensors due to evaporation of the inner filling solution or occurrence of osmotic pressure differences across the ion-selective membrane. The latter is a major factor limiting the miniaturization of ISEs. Moreover, transmembrane ion fluxes worsen detection limits and can only be suppressed with careful optimization. Not surprisingly, various efforts to eliminate the inner filling solution have been made and are briefly described in the following paragraphs to highlight the close relationship of the resulting devices to conventional ISEs (Figure 14). However, it needs to be emphasized that these solid-contact devices owe their function to exactly the same control of the sample–membrane phase boundary potential using ionophores and ionic sites as the conventional ISEs with an inner filling solution. While solid contacts have the promise to significantly enhance the

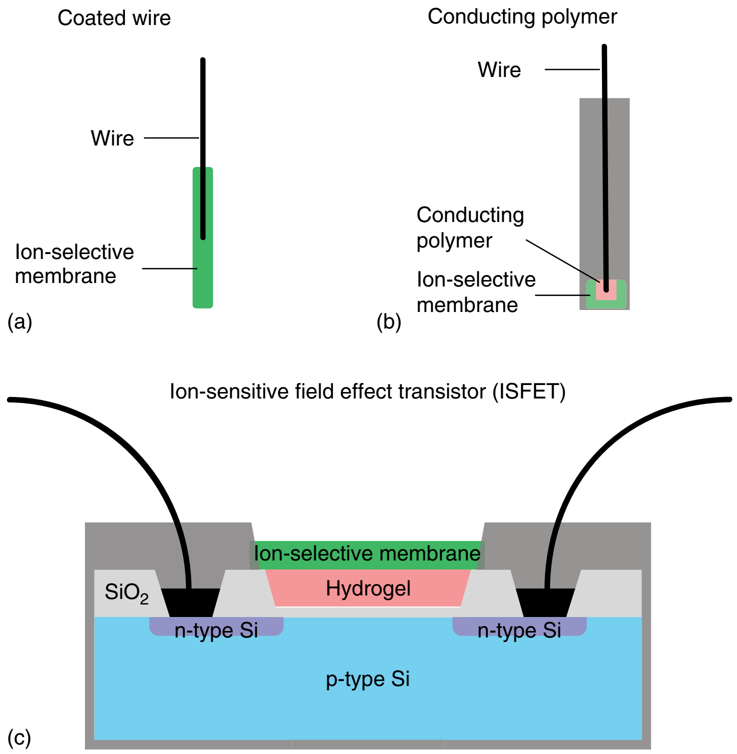

Figure 14 Potentiometric sensors with different types of internal solid contact.

reliability and extend the number of application fields of ionophore-based potentiometry, their use does not require any different host–guest chemistry than conventional ISEs.

In attempts already made in the early 1970s, the ion-selective polymeric membrane was directly applied to a metal wire.[35] From a theoretical point of view, this is an unsatisfactory situation because in all but a few exceptions these membranes contain neither a redox-active cation of the metal of which the wire is made nor an electron acceptor/donor pair that determines the redox potential. As a result, the phase boundary potential at the membrane/metal interface of most coated-wire ISEs is poorly defined. It is still not well understood why in real life freshly prepared coated-wire electrodes sometimes perform surprisingly well under circumstances when they can be recalibrated relatively frequently. However, formation of a water layer at the metal–membrane interface leads eventually to memory effects and, after delamination of the sensitive membrane, to catastrophic failure.

Another approach to eliminate the inner filling solution of conventional ISEs was introduced also in the 1970s and is based on the use of field effect transistors (FETs). These devices are referred to as ISFETs, that is, ion-sensitive FETs,[7,68,69] and belong together with enzyme FETs (EnFETs) and gas sensitive FETs to the larger category of ChemFETs (chemically sensitive FETs). In the case of the ISFET, the ISE membrane is applied to the Si_3N_4 surface of a FET, which itself is well known to be H^+ sensitive. Considerable efforts have been spent on the fabrication of hydrogel layers between the selective membrane and the FET to obtain a reproducible and stable electrode response. However, ISFETs with ionophore-doped membranes have never become a major product on the market, which appears to be mostly explained by the difficulties in controlling the hydrogel layer and preventing the ion-selective membranes from pealing off.

The realization that the interface between the ion-selective membrane and the solid contact needs to have a well-controlled phase boundary potential led in the early 1990s to the introduction of electronically conducting polymers as an electronically and ionically conducting interlayer between the ionophore-doped polymeric membrane and the underlying metal or graphite electrode.[36,70] Even though solid-contact ISEs with conducting polymer interlayers have not yet solved all problems of long-term stability, they can be considered a considerable success, are relatively easy to prepare, and have recently been shown to permit measurements with extremely low detection limits.[7] The latter can be explained by the elimination of transmembrane ion fluxes. As a result, an increasing number of research groups have been using this approach over the first decade of this century, which stands in marked contrast to the 1980s and 1990s, when only a limited number of research groups worked with solid-contact ISEs.

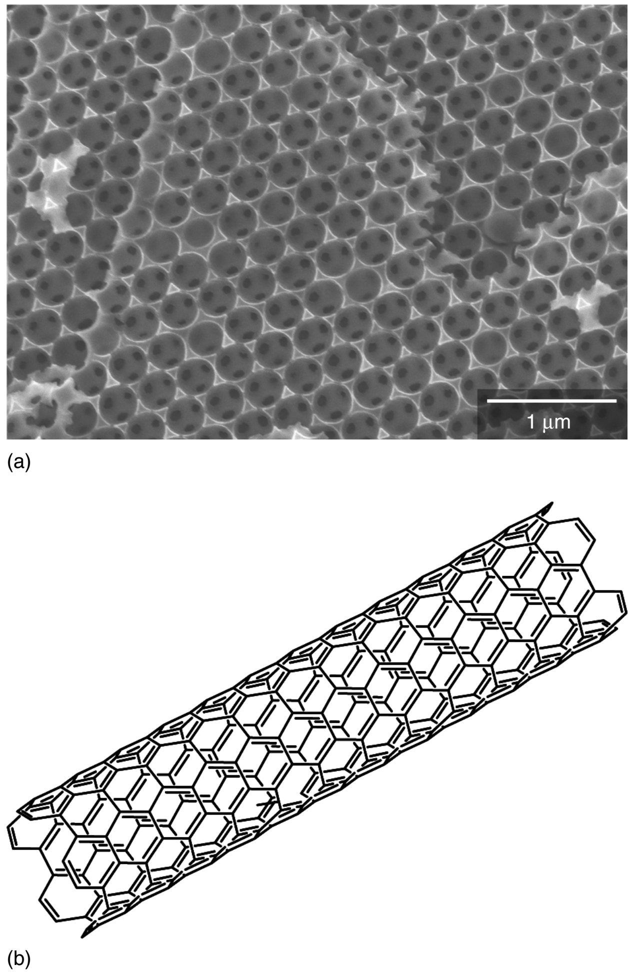

Figure 15 (a) Scanning electron microscopy image of 3DOM carbon[71] (Reproduced from Ref. 71. © ACS, 2010.) and (b) schematic representation of a carbon nanotube.

An even newer approach to solid-contact ISEs is based on carbon materials with very large surface area, that is, three dimensionally ordered macroporous (3DOM) carbon[16,38] or carbon nanotubes[37] (Figure 15). Here, the ion-selective membrane is directly infused into the carbon material. It has been shown that an extremely large surface between the two materials results in a very large interfacial capacitance,[71] which makes it very hard to polarize this interface. This appears to explain the outstanding long-term stabilities of ISE responses measured with 3DOM carbon solid contacts, which have been found to be of the order of $10\,\mu\mathrm{V\ h^{-1}}$.[38]

3.1.6 Ion-selective microelectrodes

The desire to miniaturize ISEs arises from two very different motivations. On one hand, miniaturized ISEs may be mass manufactured, lowering the cost and thereby enabling sensor networks. On the other hand, miniaturized ISEs can be used to measure in very small volumes. Examples for the latter include measurements in impaled biological cells,[33] in the eluent coming from a chromatographic column or electrophoresis capillary,[72] and in close proximity to the surface of various materials.

The earliest type of ionophore-based potentiometric microelectrodes were prepared in the mid 1970s from micrometer-sized glass pipettes, filled at the end with the ionophore-doped hydrophobic phase (Figure 16).[73,74] For speciality applications, in particular, in biochemical and medical research, these microelectrodes continue to have a variety of applications. Particularly noteworthy are their use to study intracellular ion concentrations, the release and uptake of ions into cells,[75] and their recent use as

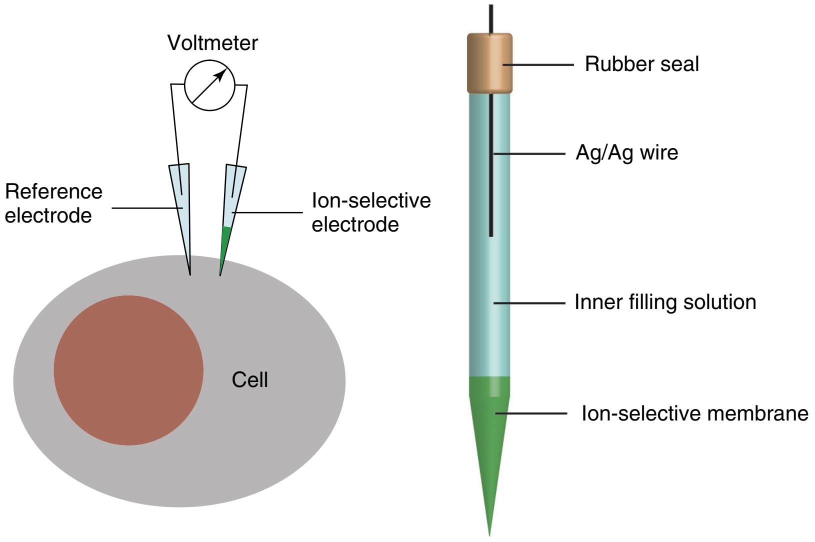

Figure 16 Ion-selective microelectrode measurement in a living cell.

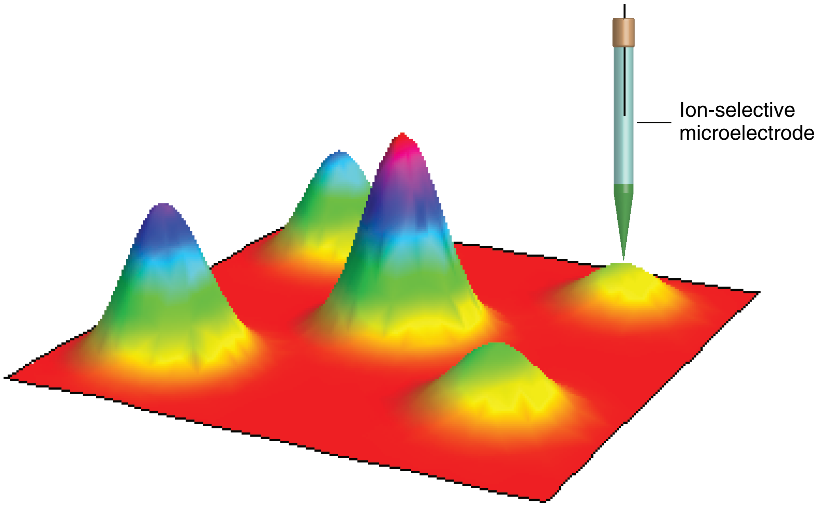

Figure 17 Ion-selective microelectrode used in scanning electrochemical microscopy (SECM) to measure profiles of ion concentrations in three-dimensional space.

the scanning probe in scanning electrochemical microscopy (SECM, see Figure 17).[76–78]

3.1.7 *Combining ionophore-based ISEs with enzymes and antibodies*

While the majority of ion receptors tested in recent years for use in ISEs are the product of organic synthesis, especially in the early history of ISEs a significant number of ionophores were obtained from biological sources. It is therefore not surprising that attempts have also been made to utilize biological compounds such as enzymes and antibodies in potentiometry.

An important advantage of enzymes is that they not only provide selectivity but also convert electrically neutral substrates into ions. One classical example is urease, which converts urea into carbon dioxide and ammonium ions, which can then be detected with an ionophore-based ammonium-selective electrode (Figure 18). The enzyme can be directly incorporated into an enzyme-containing film that is integral part of the electrode.[34] While for many years such sensors have been largely of academic interest, both urea and creatinine selective sensors recently became commercially available. A more recent example for this approach uses potentiometry for the detection of prostate specific antigen (PSA) at concentrations as low as 0.1 ng ml^{-1}.[79] First, the blood serum tested for PSA is incubated with β-galactosidase-labeled PSA tracer antibody, which permits the antibody to bind to the PSA. Upon removal of unbound antibody, 6,8-difluoro-4-methylumbelliferyl-β-D-galactopyranoside is added. The galactosidase bound through the antibody to PSA now signals the presence of PSA by hydrolysis of the galactopyranoside to give difluoromethylumbelliferone (**DiFMU**), which is detected potentiometrically in its deprotonated form. This simple

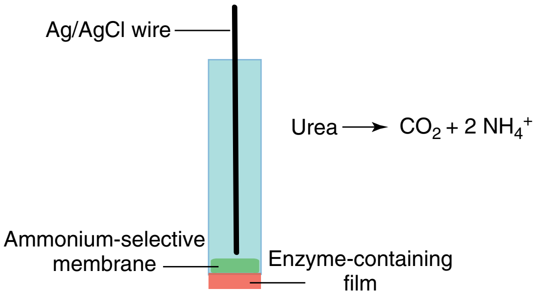

Figure 18 Urea sensor with a urease-containing film that catalyzes the decomposition of urea to give NH_4^+, which is detected with the ionophore-based NH_4^+ ISE.

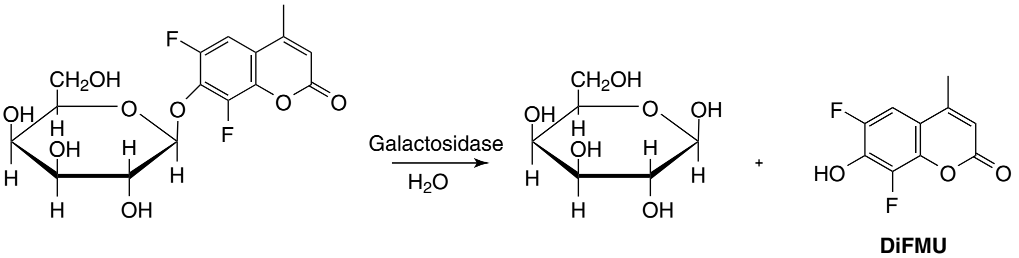

method offers an alternative to more complicated optical detection, and it is general enough that it can be modified for other potentiometric enzyme immunoassays.

To date, the majority of enzyme-based potentiometric sensors do not involve detection with an ionophore-doped selective membrane and fall outside of the scope of this chapter. The same is also true for most Severinghaus-type gas sensors, where a gas-permeable membrane covers an inner solution in which the gaseous analyte is determined with an ISE.[80] Most Severinghaus-type electrodes use a pH-sensitive glass electrode to monitor the pH of this inner filling solution. However, ammonia has been detected indirectly with an ammonium-selective ionophore-based ISEs upon protonation in that inner solution,[81] and the use of other ionophore-based ISEs for the more selective detection both in enzyme-based and Severinghaus-type ISEs is readily conceivable.

3.1.8 Related chemical sensors with an ionophore-doped sensing membrane

The concept of ionophore-doped ion-selective polymeric sensing membranes has been so successful in ISEs that it inspired several related electrochemical and optical techniques of chemical analysis. In ionophore-assisted ion-transfer voltammetry, electrical voltages are applied to the interface between aqueous solutions and ionophore-doped organic phases, and the currents caused by the resulting ion transfer across the interface are measured (Figure 19). In the closely related method of chronopotentiometry, currents are applied and the resulting changes in the electrical potential are observed. In both cases, the types of polymeric membrane matrixes and ionophores that are used are the same ones as for ionophore-based ion-selective potentiometry. However, ionic sites cannot be used in the same way to control complex stoichiometries as in the case of ISEs. Another electrochemical technique that has only been recently used in combination with ionophores is coulometry,[43,44] which is based on the integration of the observed current when applied potentials are used to transport ions from a sample into an ionophore-doped organic phase. If the samples are not too large, coulometry can be driven to exhaustion, which means that all ions of a given type have transferred from the sample into the ionophore-doped phase. The unique advantage of this approach is that it can be performed calibrationless.

Another well-developed field of chemical sensors that was originally inspired by ISEs is that of optodes,[3] which differ from ionophore-based ISEs fundamentally in that they do not rely on changes in a phase boundary potential but require after each change of sample a reequilibration that involves a complete exchange of the ionic composition of the optode membrane bulk. In the example shown in Figure 20, the optode membrane contains one ionophore for a cation of interest and a chromoionophore with a high selectivity for H^+. When exposed to samples that contain only very low concentrations of the ion of interest, the optode membrane is loaded with H^+ and exhibits the color characteristic for the protonated chromoionophore. At higher sample concentrations, the analyte cations enter the optode membrane and form ionophore complexes, and in exchange the H^+ ions transfer into the sample. As a result, the optode membrane now exhibits the color of the deprotonated chromoionophore (Figure 20).

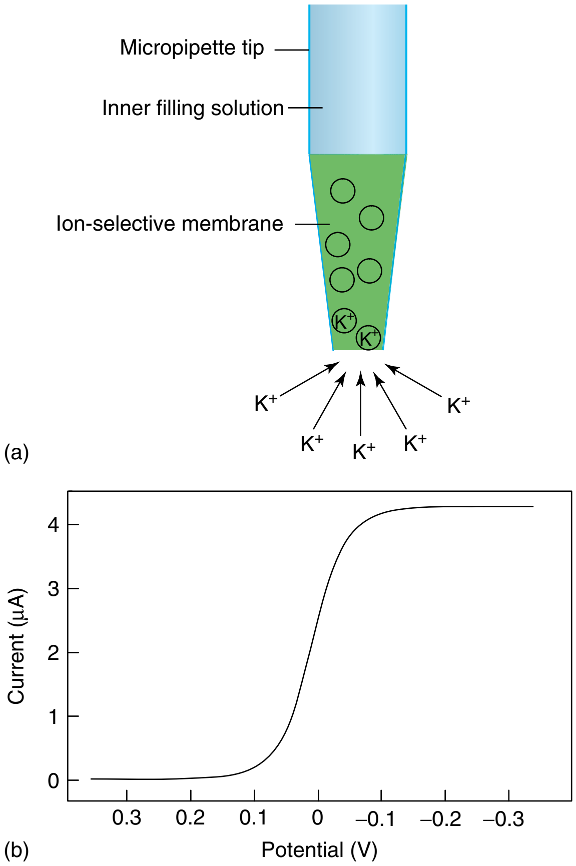

Figure 19 Ionophore-assisted ion-transfer voltammetry.

While optodes and ISEs can be prepared from the same types of ionophores, the two types of sensors differ in a number of characteristics. ISEs offer the advantage of responses over unusually large concentration ranges (10 orders of magnitude are not exceptional), whereas the optode response is limited to a much narrower range but more readily permits measurements of small concentration differences.[3] For specific applications, tuning of the basicity of the chromoionophore allows, however, to optimize the concentration range in which the optode is most sensitive. Because the optode response results from a complete

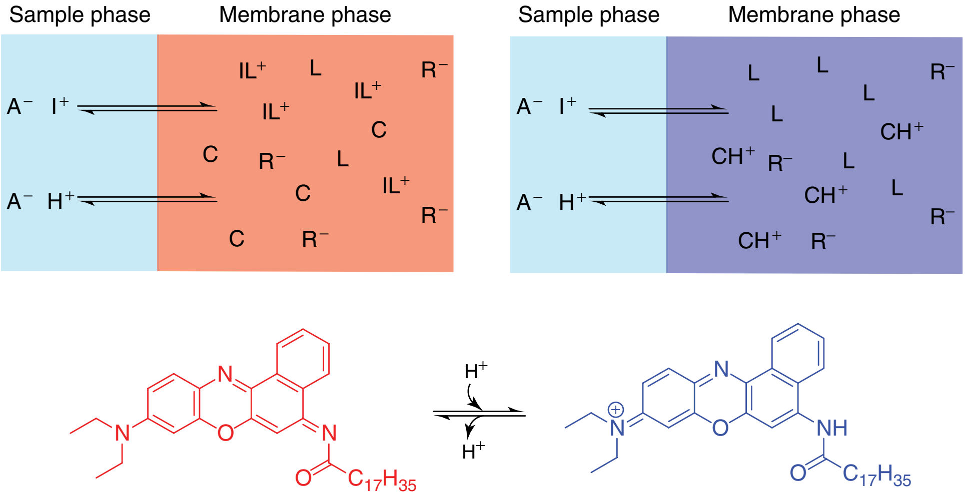

Figure 20 Ionophore-based optode based on the chromoionophore ETH5294 (C), an ionophore (L) with selectivity for the target ion I^+, and anionic sites (R^-): The sensing phase changes color when the concentration of I^+ in the sample increases, resulting in replacement of H^+ by I^+ in the optode membrane and, thereby, chromoionophore deprotonation.

exchange of the ionic content in the bulk of the optode membrane, mass transfer through the optode membrane limits the response time and makes it much slower than the ISE response. Whereas ISEs are immune to optical interferences, optodes are not affected by electrical noise. One of the biggest advantages of optodes is probably the fact that they do not require any wiring to a voltmeter and can be readily introduced in very small volumes such as biological cells. Monitoring of ionic concentrations in cells are indeed some of the most exciting applications demonstrated with optode pebbles.[82]

4 THE DESIGN OF IONOPHORES FOR ION-SELECTIVE ELECTRODES

4.1 Strength and selectivity of host–guest complexation in homogeneous phases and biphasic systems

Particularly the early years of molecular recognition chemistry, binding of guests to hosts was often investigated in organic solvents of comparatively low polarity, such as chloroform. Later on, the desire to apply this type of chemistry to systems of biological relevance has, however, motivated research into host–guest recognition in aqueous phases. Using water as a solvent brings its challenges, since both the guest and host are typically much more strongly solvated in water than in most other solvents. When partial desolvation is required to form a host–guest complex, the free energy of complex formation is reduced and complexation becomes weaker. This is particularly true for many biologically relevant ionic guests, which are very often strongly solvated in water. Justifiably, this has led to the notion that host–guest chemistry in aqueous media is much more difficult than in less polar solvents.

Occasionally, this notion has also been misinterpreted to mean that selective ion recognition in water is a much harder problem than ionic recognition in the hydrophobic membranes of ISEs. This misconception ignores the fact that ISE membranes are used to sense ions in aqueous samples, and that sensing with ISEs requires a two-step process in which the ion of interest transfers from the aqueous into the hydrophobic membrane phase and forms the complex with the ionophore in the hydrophobic ISE membrane. Importantly, this phase transfer requires desolvation because the ion leaves the aqueous phase, and is, therefore, associated with similar challenges as ionic recognition in an aqueous one-phase system.

This is easily illustrated by the case of the unfortunately still elusive highly selective sulfate ISE. Because of the very strong hydration of sulfate in water, it is unquestionably much harder to form sulfate complexes in water than in less polar solvents (Figure 21). However, the strong solvation of sulfate in water also makes it very difficult to make a sulfate ISE with high selectivities over ions that are less strongly hydrated, such as chloride or nitrate. To obtain an ionophore-based ISE with a selectivity for sulfate over chloride, it is not sufficient that the ionophore forms a sulfate complex that is more stable than its complex with chloride. Instead, sulfate complexation must be much stronger so that the difference in the free energies of complexation of the two ions compensates for the fact that sulfate is much more strongly hydrated than

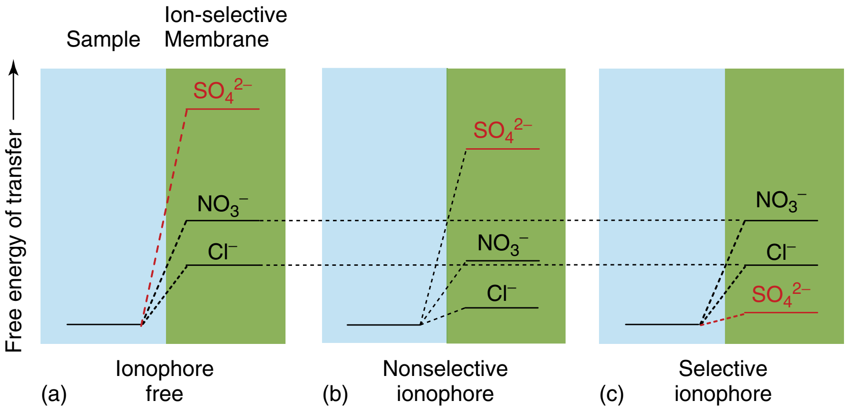

Figure 21 Free energy of transfer of SO_4^{2-} into ion-selective membranes: (a) sulfate transfer into the ionophore-free membrane is energetically most unfavorable due to large hydration energy; (b) a nonselective ionophore reduces the phase transfer energy for all ions equally; (C) the selective ionophore facilitates sulfate transfer selectively.

chloride. This is not a challenge unique to ISEs, but it is common to all biphasic systems, which also include solvent extraction, biphase catalysis, and some types of membrane separations.

The above example also illustrates that the most important characteristic of good ionophores for use in ISEs is not binding strength but selectivity. For example, a 10-fold increase in the binding constant for sulfate obtained by optimization of the ionophore structure will not change the selectivity of an ISE over chloride if the binding constant for chloride is also increased 10-fold. Also, whereas strong binding is a requirement for good selectivity, too strong binding is not desirable because it can result in the extraction of the primary ion along with an ion of opposite charge sign from the aqueous sample into the bulk of the sensing membrane.[52] Consider, for example, a chloride ISE membrane based on an electrically neutral, strongly binding chloride ionophore and 50 mol% cationic sites responding to increasing concentrations of KCl in the aqueous sample. Within the range of the linear (Nernstian) response to the logarithm of the chloride activity, the bulk of the ISE membrane contains free ionophore and ionophore complexes in a 1 : 1 ratio, and the charge of the latter is balanced by the cationic sites. The bulk composition of the ISE membrane does not change until at very high concentrations the ISE looses its ability to respond to only ions of one charge sign. At this point, bulk extraction of KCl from the aqueous into the membrane phase results in conversion of all free ionophore to the chloride complex, and the K^+ concentration in the membrane bulk becomes 50 mol% relative to the total ionophore concentration. At the onset of bulk extraction, the upper detection limit of the ISE is reached, and it ceases to respond to chloride. This effect is typically referred to as Donnan failure or the loss of permselectivity.[83,84] A high stability of the K^+ complex will favor Donnan failure and will thereby lower (i.e., worsen) the upper detection limit of the ISE (Figure 22).

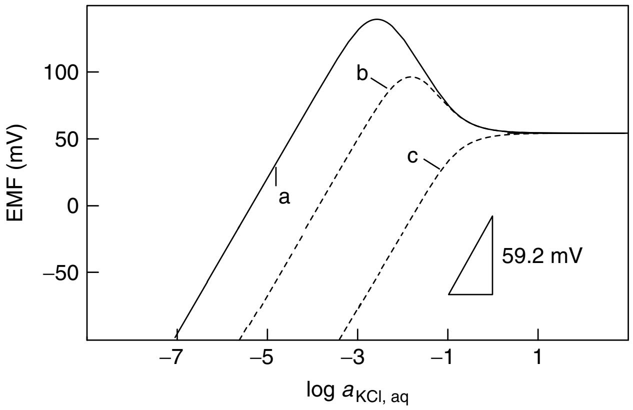

Figure 22 Increases in the stability of the complex between the target ion (here K^+) and the ionophore increase selectivity but also reduce the upper detection limit of an ISE due to coion interference (binding constant of K^+-ionophore complex: a > b > c).

4.2 Ionophore-based ion-selective electrodes for pH

Because of the key role of water for all living organisms, the measurement of pH is arguably the most important application of potentiometry. This is underscored by the fact that the pH is not defined on the basis of the hydrogen ion concentration but by its activity, which is readily accessible only by potentiometry.[85,86] In the majority of cases, such measurements are performed with commercially available glass electrodes.[23] The use of glass as the sensing membrane has a number of disadvantages, though. Proteins and other biological materials readily adsorb to glass, which requires frequent electrode cleaning. Even the speciality glasses used for pH glass electrodes have a very high electrical resistance and are, therefore, difficult to be miniaturized. Moreover, the use of thin glass membranes as dictated by the high electrical resistance also makes glass electrodes prone to breakage, which is particularly undesirable in the food industry and in *in vivo* measurements. This has lead to a significant interest in the development of ionophore-based ISEs for pH.

From a host–guest chemistry point of view, H^+ ionophores are as simple as it gets. While a remarkable variety of H^+ ionophores have been tested,[4] simple trialkylamines and pyridine derivatives that bind the hydrogen ion in a monodentate fashion are suitable for most applications. Ionophore-based pH electrodes illustrate in exemplary fashion that finding a compound that forms a very stable complex with the target ion is not sufficient for the preparation of a good ISE. Tridodecylamine (**H^+-I**),[87] for example, binds H^+ strongly and permits pH measurements up to pH 11, where the hydrogen ion activity is so low that the alkali metal cations often used to prepare solutions of such high pH are starting to interfere. However, the strong binding of the hydrogen ion to this ionophore also promotes Donnan failure (Section 4.1 and Figure 22) at low pH, that is, the coextraction of hydrogen ions and counteranions from the aqueous sample into the sensing membrane and the concomitant loss of the linear response to pH. This limits the use of ISEs based on **H^+-I** to samples of pH 4.5 and higher. For measurements at lower pH, ionophores that form less stable H^+ complexes are needed, such as **H^+-II**, which is suitable for the pH range from 0 to 8.[88] Evidently, the smaller binding constants limit the selectivity at higher pH.

The membrane matrixes doped with these ionophores have a strong effect on selectivity. The useful pH range is reduced at higher pH by polymers or plasticizers with functional groups that interact with interfering cations, and polymers. Plasticizers and ionic sites that stabilize counteranions in the sensing membrane facilitate Donnan failure at the lower end of the pH range. Evidently, inert matrixes are preferred as they provide the widest measurement ranges.[89] Since perfluorocarbons are the least polar and least polarizable condensed phases known, they are, expected to offer

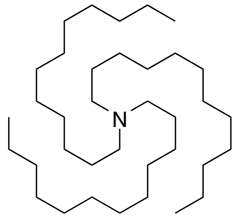

H^+-I

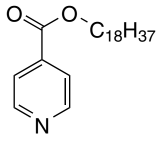

H^+-II

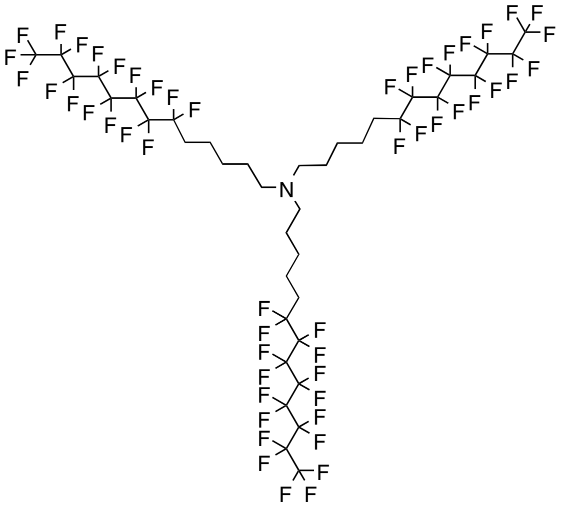

H^+-III

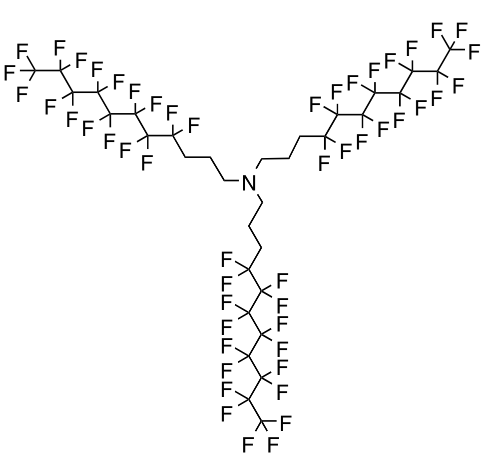

H^+-IV

the weakest stabilization to interfering cations and counteranions. Indeed, H^+ selective ISEs with fluorous membranes and fluorophilic ionophores are among the most selective of all.[62,67] The highest selectivity was observed for **H^+-III**, whose -$(CH_2)_5$- spacers shield the H^+-binding nitrogen from the three strongly electron withdrawing perfluoroalkyl groups. Surprisingly, the -$(CH_2)_3$- spacers of **H^+-IV** are already too short for sufficient shielding of the nitrogen center. While the selectivity for H^+ over Na^+ of ISEs based on **H^+-III** is larger than 13 orders of magnitude and cannot be determined accurately because it is not possible to prepare solutions with Na^+ concentrations that are sufficiently high to cause interference, the H^+ over Na^+ selectivity of ISEs based on **H^+-IV** is only $10^{9.6}$-fold. Using the recently developed ISE theory, this can be explained quantitatively by a pK_a of **H^+-III** in the fluorous phase of 15.4, which is 5.6 pK_a units larger than for **H^+-IV**.[67]

4.3 Ion recognition based on ion–dipole interactions

4.3.1 Ion-selective electrodes for alkali metal cations

Attractive interactions that can be used to design ionophores include ion–dipole interactions, hydrogen bonds, ligation to metal cations, and the formation of covalent bonds. Ligation of an anion to a metalloporphyrin or covalent binding of carbonate to trifluoroacetophenone ionophores are examples of guest recognition based on a monotopic interaction. However, more often than not, ISE ionophores bind ions through multitopic interaction. This is particularly true for the large class of cation receptors that interact with their guests by ion–dipole interactions. Some of the earliest and very successful examples include natural compounds such as the antibiotics valinomycin, monactin, and nonactin already mentioned above (Figure 3), while the majority of recent reports on ISEs with ionophores of this class describe the use of synthetic compounds. Because it would be well beyond the scope of this chapter to discuss this field comprehensively, examples of ionophore-based ISEs for K^+, Na^+, and Li^+ will be discussed in this section to the extent that they represent different types of ionophore design. However, it must be emphasized that much more work has been performed in this field, and ISEs have been developed for over two dozen inorganic cations. In particular, decades of research have been made to improve the design of ISEs for the clinically relevant ions Ca^{2+} and Mg^{2+},[90] and numerous ISE have been reported for many heavy metal ions.[4,91]

The cyclic peptide valinomycin binds to K^+ through 6 of its 12 carbonyl groups. Sensors based on this ionophore exhibit remarkable selectivity, such as a $10^{4.5}$-fold selectivity over Na^+.[17] This selectivity permits analysis in blood and urine, a purpose for which ISEs based on this ionophore continue to be used widely in large throughput ("mainframe") clinical chemistry analyzers. Disadvantages of valinomycin include, however, a limited solubility in polymeric matrixes of lower polarity and a relatively low hydrophobicity.[92]

Most synthetic alternatives to valinomycin take advantage of ether oxygens that bind to K^+. Earlier examples of monocyclic crown ethers have given way to more selective bis-15-crown-5 ethers that bind the K^+ in a sandwichlike fashion. **K^+-II**,[93] which provides for a $10^{3.7}$-fold selectivity over Na^+, is an excellent example. The individual 15-crown-5 macrocycles are too small to bind the K^+ in their center. As a result, the K^+ ion comes to lie in between the two 15-crown-5 macrocyclic rings, providing for a total of 10 oxygen–ion interactions. Ions smaller than K^+ cannot take advantage of interactions with all these ether oxygens, while ions larger than K^+ would benefit from interactions with the additional ether oxygens in larger crown ethers. The selectivity of ISEs based on bis-15-crown-5 ethers is, however, limited by the large conformational freedom of these ionophores. Among several efforts to restrict the conformational freedom of the ionophore and thereby increase size selectivity, the development of bridged calix[4]arene-crown-5 compounds such as **K^+-II**, which was reported to have a $10^{4.2}$-fold selectivity over Na^+, is particularly noteworthy.[94]

Similar trends as for the K^+ ionophores can also be seen for Na^+. Very early examples of ISEs based on

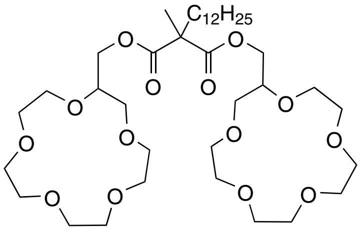

K^+-II

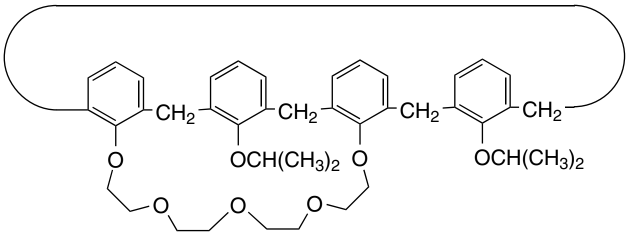

K^+-III

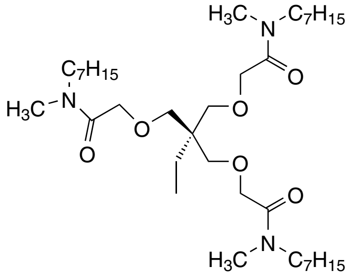

Na$^+$-I

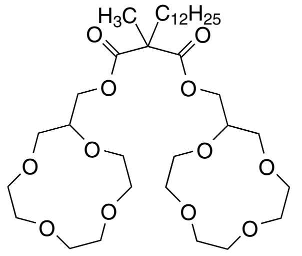

Na$^+$-II

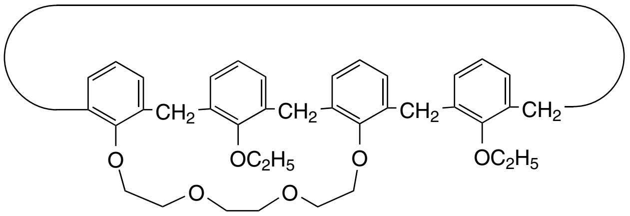

Na$^+$-III

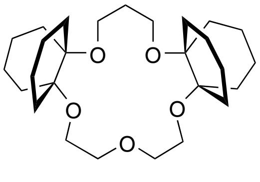

Na$^+$-IV

antibiotics were soon followed by more selective synthetic ionophores binding Na$^+$ with multiple carbonyl groups. A particular successful ionophore of that generation is **Na$^+$-I** ($10^{2.3}$-fold selectivity over K$^+$), which has been used successfully for intracellular measurements despite the high K$^+$ concentrations in this environment.[31] Many ionophores introduced subsequently were macrocyclic crown ethers with oxygens as the recognition sites, as in the case of the K$^+$ ionophores too. With its smaller size, Na$^+$ fits well into 15-crown-5. Not surprisingly, the most successful bis-crown ether ionophores have two 12-crown-4 macrocyclic rings, between which the Na$^+$ is bound with eight ion–ether interactions (e.g., the commercially successful **Na$^+$-II** with a $10^{2.1}$-fold selectivity over K$^+$).[95] As in the case of K$^+$ selective bis-crown ethers too, the conformational freedom of the bis-12-crown-4 ethers is large, which limits the achievable selectivity, and as in the case of K$^+$ ISEs too, extremely successful bridged calix[4]arenes have been proposed. **Na$^+$-III** with a $10^{5.3}$-fold selectivity over K$^+$ is an outstanding example.[96] An alternative approach relying largely on steric repulsion to exclude larger ions and prevent the formation of complexes between one ion and two ionophores is exemplified by **Na$^+$-IV** ($10^{3.0}$-fold selectivity over K$^+$).[97]

Interest in the analysis of Li$^+$, the smallest alkali metal ion, using ISEs stems predominantly from its use as a mood-stabilizing drug.[4,98] The most important interferent in clinical measurements is Na$^+$, which occurs in blood in a concentration of approximately 140 mM. Early work with diamide ionophores[4] such as **Li$^+$-I,** which forms 1 : 2 complexes with Li$^+$, found selectivities ($10^{2.3}$-fold selectivity over Na$^+$) barely permitting the first successful measurements in blood.[99,100] In 1987, the first commercial clinical analyzer measuring Li$^+$ with ISEs became available.[101] While various approaches were taken to improve the selectivity over Na$^+$, the most successful one is arguably the one in which 1,4,8,11-tetraoxacycolotetradecane was decorated with bulky substituents hindering the formation

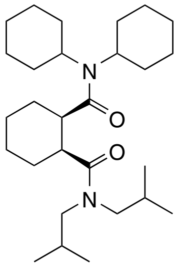

Li$^+$-I

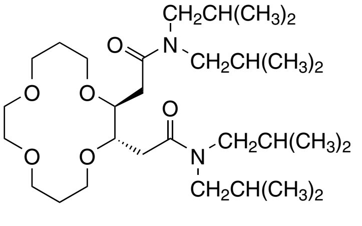

Li$^+$-II

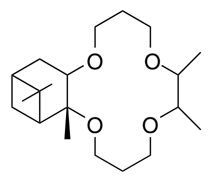

Li$^+$-III

of 1 : 2 complexes and inhibiting the binding of larger ions. The highest potentiometric selectivity was reported for **Li^+-II** ($10^{3.3}$-fold over Na^+),[102] but similar selectivities were also found for several other compounds.[103] Interestingly, a more than 10^4-fold selectivity but a slow response was reported for the sterically even more hindered **Li^+-III**.[103]

A fair number of ionophore-based ISEs with selectivities for Rb^+ and Cs^+, the two largest alkali metal cations, have also been described. In some of these cases, the potentiometric selectivities suggest that the ionophore binds the target ion selectively. However, in a number of cases such evidence is missing. Since Cs^+ has the lowest free energy of hydration of all alkali metal cations, even an ionophore-free ion-exchanger membrane will exhibit selectivity for Cs^+ over the other alkali metal cations. To show evidence for selective recognition of Cs^+ by the ionophore, the selectivity of an ionophore-based ISE for Cs^+ has be higher than for an ionophore-free ion-exchanger ISE based on a membrane containing the same membrane components but no ionophore (but including ionic sites), a control experiment that is unfortunately too often not reported.

4.3.2 Ion-selective electrodes for NH_4^+

Because of the key role of NH_4^+ in various biological processes, the direct measurement of this ion is important for clinical and environmental analyses. Ammonium concentrations in food also provide a measure of freshness. Moreover, various enzymes catalyze the deamination of numerous organic compounds, which makes NH_4^+ selective ionophores also of interest for enzyme-based ISEs (Section 3.1.7). For all these reasons, there has been a continued interest in the development of ionophore-based ISEs for NH_4^+.

For many years, almost all the work on NH_4^+ ISEs focused on the macrocyclic antibiotics nonactin (**NH_4^+-I**) and monactin (**NH_4^+-II**), see Figure 3.[4,104] While the type of sensing matrix has some effect on the selectivities of ISEs based on these ionophores, an approximately 10-fold selectivity over K^+ and an approximately 100-fold selectivity over Na^+ is characteristic for these sensors. Only in recent years several interesting alternatives have been proposed. Significant improvements of the selectivity of either Na^+ or K^+ have been obtained by use of rigid crown ethers with bulky substituents that block complexation with larger ions (e.g.,**NH_4^+-III**),[105,106] a

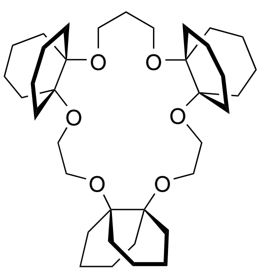

NH_4^+-III

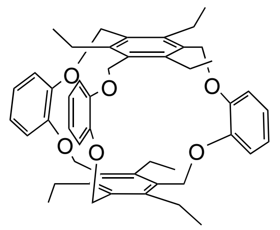

NH_4^+-IV

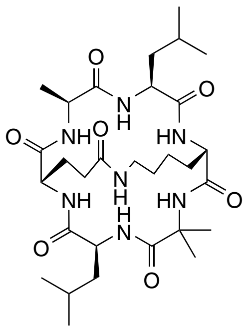

NH_4^+-VI

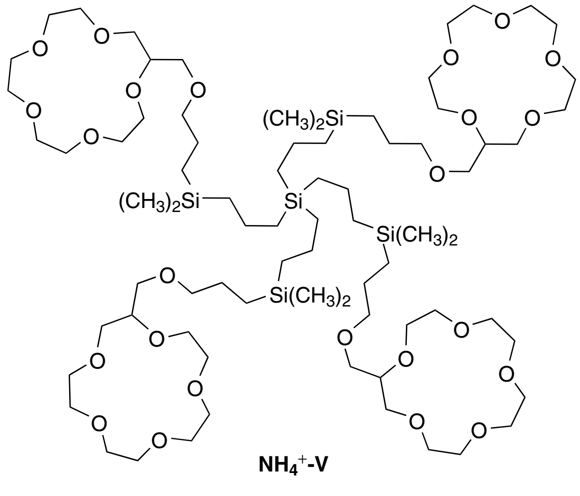

NH_4^+-V

strategy similar to the one described above for Li^+ and Na^+, A 1000-fold selectivity over Na^+ was also achieved with the macrobicyclic **NH_4^+-IV**, which was explained by both hydrogen bonds to the ether oxygens and cation–π interactions.[107] In comparison, the dendrimer **NH_4^+-V** with four 15-crown-5 groups has only a low level of host preorganization, which makes the reported nearly thousand fold selectivity over Na^+ rather surprising.[108]

A report on the macrobicyclic peptide ionophore **NH_4^+-VI** illustrates some of the often unexpected challenges of ionophore design. Molecular modeling was used for the design of this ionophore, and did result in a selectivity close to the one for monactin- and nonactin-based ISEs, but the poor solubility of **NH_4^+-VI** proved to be an unexpected problem.[109]

4.3.3 *Ion-selective electrodes for alkaline earth metal cations*

While there has been only a limited interest in ionophore-based ISEs for Be^{2+}, Sr^{2+}, and Ba^{2+},[4] the development of Mg^{2+} and Ca^{2+} ISEs suitable for measurements in blood samples has been for several decades one of the most competitive topics in the field of ion-selective potentiometry. Success came much faster for Ca^{2+} than for the smaller and more hydrophilic Mg^{2+}, for which ionophore-based ISE were finally introduced in clinical analyzers in 1994.[91] This can be at least partially explained by the fact that, as a result of the stronger hydration of Mg^{2+}, the use of a hypothetical ionophore that binds Mg^{2+} and Ca^{2+} equally strong would result in an ISE with selectivity for Ca^{2+} over Mg^{2+}. Therefore, binding of Mg^{2+} by the ionophore has not only to be selective over Ca^{2+}, but it also has to compensate for the difference in the free energies of ionophore-unassisted phase transfer from the aqueous into the sensing membrane. Analogous problems arise in the development of other strongly hydrophilic cations (e.g., Li^+) and anions (e.g., sulfate and phosphate).

Because of the intense interest in Mg^{2+} and Ca^{2+} ISEs, a lot of work was performed in which the structures of ionophores with different levels of preorganization were varied very methodically by use of substituents with different levels of bulkiness and electronegativity.[4] Arguably, this work contributes to the most sophisticated examples in the field of supramolecular chemistry. Unfortunately, because a lot of this work was performed before methods for the determination of complex stabilities in ISE membranes became available, the majority of this work was directed by the experimentally observed potentiometric selectivities alone. Complex stabilities have only been determined much later for a few selected examples.

Ionophores that meet the demands of clinical chemistry and biochemical and physiological research had been developed by the end of the 1990s. More recent work has mostly focused on ionophores that are more readily available but have not led to major breakthroughs in selectivity. Since the history of Ca^{2+} and Mg^{2+} ISEs has been reviewed,[4,110] this chapter will only briefly highlight some of the ionophores that represent the current state of the art.

Despite their apparently low level of host preorganization, the noncyclic amide ionophores **Ca^{2+}-I** (ETH 1001) and **Ca^{2+}-II** (ETH 129) continue to be the default ionophores for many real-life applications. While the former is suitable for measurements in blood serum,[111] the latter has a better selectivity over Na^+ and K^+ and is more suitable for intracellular measurements.[112] However, ionophores with higher selectivities have recently been developed. Two of the most elaborate examples that only resulted from painstaking optimization include the diazacrown ethers **Ca^{2+}-III** and **Ca^{2+}-IV**.[113] In the complexes of these two ionophores with Ca^{2+}, the metal ion is situated in the crown ring, and the two pendants bind to the Ca^{2+} from the top and bottom.

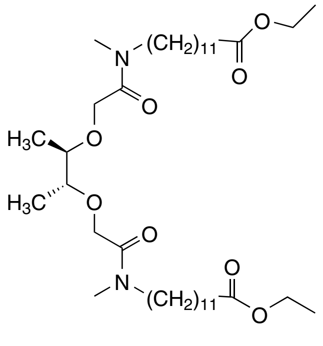

Ca^{2+}-I

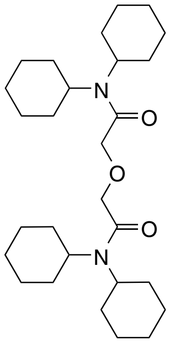

Ca^{2+}-II

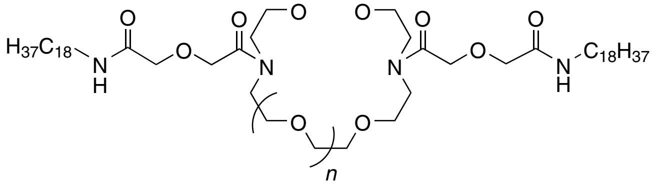

Ca^{2+}-III: $n = 2$
Ca^{2+}-IV: $n = 1$

The structures of the most successful Mg^{2+} ionophores have a strong resemblance to those of Ca^{2+} ionophores. While early work with diamide ionophores for Mg^{2+} was also performed, the most selective noncyclic ionophores for Mg^{2+} are the triamides **Mg^{2+}-I** and **Mg^{2+}-II**.[114,115] A systematic optimization similar to the one for **Ca^{2+}-III**

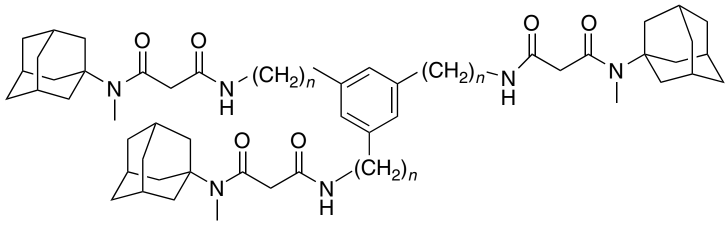

Mg^{2+}-I : $n = 4$

Mg^{2+}-II : $n = 5$

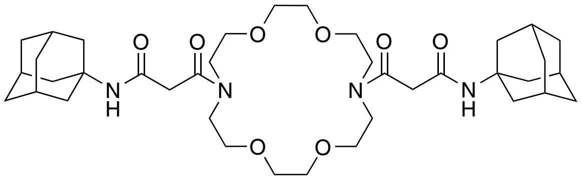

Mg^{2+}-III

and **Ca^{2+}-IV** resulted in ISEs based on **Mg^{2+}-III**, which exhibits a 300-fold selectivity for Mg^{2+} over Ca^{2+}.[113]

4.3.4 Ion-selective electrodes for transition metal and lanthanide cations

Even though the number of transition metal and lanthanide cations is very large, the day seems to be soon approaching when an ionophore-based ISE will have been reported for the detection of every one of these cations. Arguably, with notable exceptions, the overall level of sophistication of the ionophore design used for these sensors has not yet reached the level that it has in the case of the ISEs for alkali and alkaline earth metal cations discussed above.

Many early investigations on ISEs for heavy metal cations (e.g., Cu^{2+}, Ag^{+}, Zn^{2+}, Cd^{2+}, Hg^{2+}, Pb^{2+}, and $UO_2{}^{2+}$)[4] were inspired by ionophores that were already readily available from other type of research, such as fundamental studies in inorganic chemistry or the development of chelating reagents for solvent extraction. The same is often true too for ISEs reported to have selectivity for specific lanthanide cations, a field that has gained increased popularity over the past ten years. In a fair number of cases, the ionophores have not been specifically designed for use in ISEs, and suffer from insufficient hydrophobicity. Also, many of these ISEs were described before the theory was developed to permit nano- and picomolar detection limits (Section 3.1.3 and Figure 10). As a result, the lower detection limits observed in most of these studies were not low enough to permit analysis of real-life environmental and biological samples, which limited the enthusiasm for fine tuning of the selectivity to meet the needs of actual applications by ionophore optimization as described in Sections 4.3.1 and 4.3.3 earlier. Similarly, numerous older studies are hard to interpret quantitatively on the basis of modern ISE theory because either selectivities have not been determined adequately, control experiments with ionophore-free ion-exchanger selectivities have not been reported, or ionophore-site ratios have not been optimized for optimum selectivity.

The key type of interactions used in almost all the ionophores for transition metal and lanthanide cations are ion–dipole interactions. However, since these cations vary widely in their hardness as Lewis acids,[116] the character of the cation–ligand interactions ranges from mostly electrostatic for hard Lewis acids to mostly covalent for soft Lewis acids. For the latter, ligands with functional groups that are soft Lewis bases, such as amines, pyridines, thioethers, and thiocarbonyls are common. Another feature peculiar to ISEs for this group of analytes is the fairly larger number of electrically charged ligands. This is undoubtedly the result of the use of host compounds first developed for solvent extraction, where many chelating reagents are electrically neutral when fully deprotonated but bind metal cations as mono- or polyanionic species. Unfortunately, the efficient use of electrically charged ionophores is not as easy as that of electrically neutral ionophores.[52,53] As a result, the full impact of the ionic site theory needed to put electrically charged ionophores to optimum use (Sections 4.2 and 5.2) has yet to happen. Numerous recent studies using such ionophores still do not take full advantage of the selectivity improving variation of the molar ratio of ionic sites and ionophore.

However, combining the common ionophore design strategies of host rigidity to enhance ion size selectivity and bulky substituents to control complex stoichiometry with the inherent selectivity provided by soft coordinating groups permits exceptional selectivities. Therefore, in spite of the lesser level of fine tuning that has been performed, heavy metal ion ISEs are among the most selective ISE reported to date. Their comprehensive discussion is well beyond the scope of this chapter, and only a few will be mentioned here. From a historical perspective particularly noteworthy is **Pb^{2+}-I**, which was used in 1997 to demonstrate for the first time that picomolar detection limits can be achieved with ISEs with a metal ion-buffered inner filling solution.[9] Other examples of extremely selective ISEs include those based on the ionophores **Ag^{+}-I**[117] and **Ag^{+}-II**.[16] While the former gives the most selective Ag^{+} ISEs based on nonfluorous membranes reported to date, the latter is a fluorophilic ionophore that provides selectivities over many ions by an additional two orders of magnitude (e.g., $\log K^{\mathrm{pot}}_{\mathrm{Ag,J}}$ for K^{+}: -11.6; Pb^{2+}: -10.2; Cu^{2+}: -13.0; Cd^{2+}: -13.2). Evidently, this is another example of the extremely high selectivities that result when the ionophores are very selective and the transfer of interfering ions into the sensing membrane is disfavored by the extremely low polarity and polarizability of fluorous phases (for other examples, see H^{+} sensors in Section 4.2 and the carbonate sensors in Section 4.5). Such high selectivities are also the key to low detection limits, and indeed **Ag^{+}-II** has been used to demonstrate a detection limit for Ag^{+} of 4.1 ppt, which is the lowest detection limit obtained so far for an ionophore-based Ag^{+} ISE.

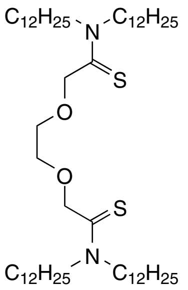

Pb^{2+}-I

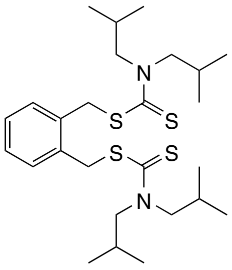

Ag^{+}-I

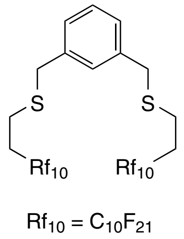

Ag^{+}-II

As the work with **Pb^{2+}-I** first demonstrated, accurately determined (so-called "unbiased") selectivity coefficients[45] can be much larger than what had been reported in the earlier literature. This is particularly true for many reports on the selectivity of transition metal cation ISEs made before 1997, which need to be interpreted carefully. Because of this and because of the new possibilities that nano- and picomolar detection limits offer, it appears that despite a lot of work that has been done in the field of transition metal and lanthanide cation ISEs, this field has still a large potential to grow and perform much better than it was the case in the past.

4.4 Anion recognition based on hydrogen bonds

While cation–dipole interactions dominate in the recognition of inorganic cations, anion–dipole interactions have been rarely taken advantage of in the design of ionophores for ISEs. Instead, a number of different interaction types have been used to develop ionophores for anions. These include hydrogen bonds, coordination to metal centers, and covalent bonds.

Among the earliest examples of electrically neutral ionophores for ISEs that bind inorganic anions through multiple hydrogen bonds were ionophores with two thiourea bonds, such as **SO_4^{2-}-I** and **Cl^{-}-I**.[118,119] More recent examples include increasingly complex structures designed to improve host–guest preorganization, such as urea-functionalized calix[4]arenes (e.g., **CO_3^{2}-I**).[120]

Not surprisingly, binding strengths increased when the host preorganization was increased and when the hydrogen-bond donor strength was increased. The latter can be achieved, for example, by switching from a urea to a thiourea group or by using more strongly electron withdrawing substituents attached to the hydrogen-bond donating group.[121] However, this concept has its limitations, as an increased hydrogen-bond donor strength typically also comes along with an increased acidity. Loss of a proton reduces the number of hydrogens available for hydrogen bonding and, in the case of an electrically neutral ionophore, results in a negatively charged compound that for electrostatic reasons is even less likely to bind an anion.[63]

One of the biggest complications in the use of a slightly acidic ionophore for anions is that such deprotonation does not only depend on the pH but also the anion and cation concentrations in the sample. To understand this, let us consider for simplicity an ISE membrane that contains an electrically neutral but acidic ionophore that binds SO_4^{2-} with 1 : 1 stoichiometry and an equal amount of a tetraalkylammonium ions as ionic sites (Figure 23). When exposed to sulfate solutions of moderately low pH, all the ionophore will be in its electrically neutral state, and half of the ionophore will form a complex with SO_4^{2-} while the other half is in its noncomplexed form (left hand side of Figure 23). If the sulfate concentration of the aqueous solution is kept constant but the pH is raised significantly by addition of KOH, the composition of the ion-selective membrane can be changed by deprotonation of the ionophore. Since deprotonation of the ionophore in the bulk of the ISE membrane and loss of the proton into the aqueous

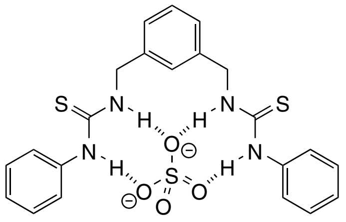

SO_4^{2-}-I

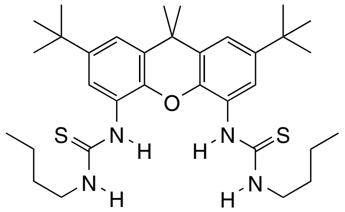

Cl^--I

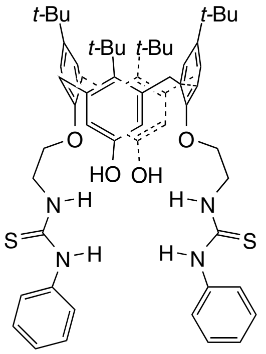

CO_3^{2-}-I

solution cannot happen in disregard of the electroneutrality requirement of the ISE membrane bulk, ionophore deprotonation will be accompanied by K^+ transfer into the sensor membrane (top right of Figure 23). What is happening is ion exchange. It follows that ionophore deprotonation will not happen at the pH at which the ionophore would be deprotonated if it were present in the aqueous phase, but that instead the pH at which this ion exchange occurs depends on (i) the pK of the ionophore in the membrane phase, (ii) the K^+ concentration in the aqueous sample, (iii) the free energy of K^+ transfer from the aqueous into the membrane phase, and (iv) the stability of a possible complex in the membrane between the K^+ and the negatively charged, deprotonated ionophore. Therefore, the pH at which ionophore deprotonation occurs changes (a) if NaOH is used to raise the pH instead of KOH, or (b) if the aqueous solution contains in addition to sulfate and KOH also another source of K^+ that raises the K^+ concentration in the aqueous sample. To make things even more complicated, ion exchange is not the only mechanism that can lead to ionophore deprotonation. Consider again the membrane of the above composition, this time exposed to a sulfate solution of a pH that is relatively high but not too high, so that all the ionophore is again in its electrically neutral state, and half of the ionophore is in the form of a complex with SO_4^{2-}. Lowering the sulfate concentration in the aqueous solution at constant pH may now result in the transfer of H^+ and SO_4^{2-} (in a 2 : 1 ratio) from the sensing membrane into the sample (Figure 23b). In this case, coextraction rather than ion exchange occurs. In either case, the observation of the solution pH at which the ionophore in the sensing membrane is deprotonated is meaningless if this experiment is performed with sulfate-free aqueous solutions. Unfortunately, the complexity of such systems has been underestimated, and too many poorly designed experiments have been described in the ISE literature.

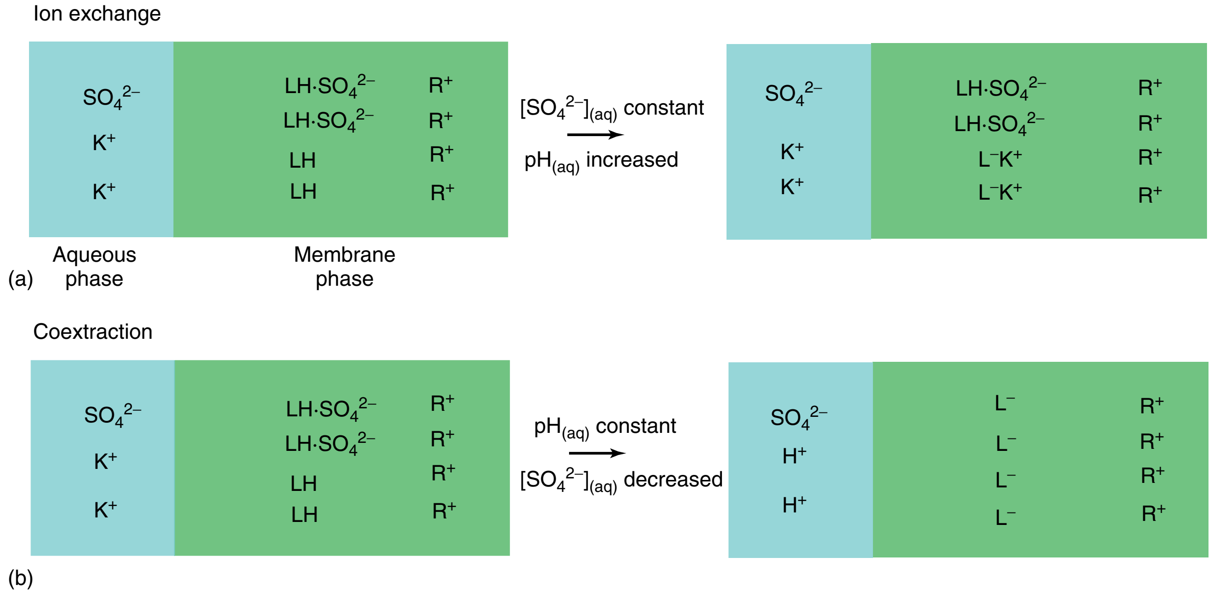

Figure 23 Ion exchange and coextraction in membranes with an ionophore that can be deprotonated.

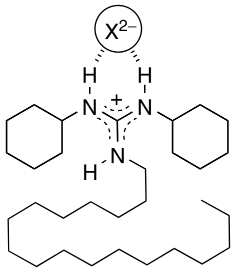

SO_4^{2-}-II

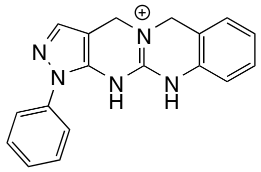

HSO_3^--I

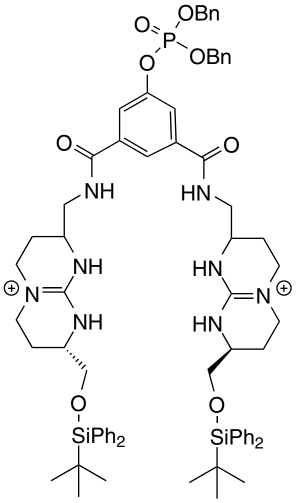

SO_4^{2-}-III

Very similar problems are often encountered for ionophores with positively charged, protonated groups that form hydrogen bonds to anionic analytes. Examples include protonated macrocyclic amines and ionophores with guanidinium groups (see also Ref. 4). The complexation chemistry of such compounds in the aqueous phase is among the early highlights of host–guest, but it has been difficult to use such receptors successfully in ionophore-doped ISEs. To minimize such problems, very basic ionophores are preferable, but even the properties of ISEs based on ionophores with guanidinium groups, such as **SO_4^{2-}-II**,[122] **HSO_3^--I**,[123] and **SO_4^{2-}-III**[124] are often difficult to explain and control.

4.5 Anion receptors with metal centers

Among the different interaction types that have been taken advantage of to develop ionophores for anions, the formation of coordination bonds between the analyte anion and a metal center of the ionophore is arguably the most common one. It was also one of the first host–guest chemistry concepts used successfully in ISEs for anions. Among the first such sensors were tin-organic receptors for chloride-selective electrodes (e.g., **Cl^--II**)[125] and nitrite-selective electrodes with lipophilic derivatives of vitamin B_{12} with a Co(III) center (**NO_2^--I**).[126] From the point of view of real-life applications, one of the most successful ISEs for anions is the one with a manganese(III) tetraphenylporphyrin as ionophore (**Cl^--III**),[127] which was successfully applied to measure chloride in blood serum and intracellular environments. In the mean time, ionophores with a very large number of different metal centers have been investigated; Mn(III), Co(III), Ga(III), Ge(III), Mo(V), Ru(II), Rh(III), Pd(II), In(III), Sn(IV), Hf(III), Hg(II), and U(VI) are examples of many (see Refs 4 and 85). Strategies for the use of these ionophores in a manner that gives the highest possible potentiometric selectivities can be rather involved and have partially been developed only recently.[53, 128, 129] Key challenges are the limited chemical stability of some of these ionophores, and the proper control of their stoichiometries with the target ions on one hand and interfering ions on the other hand.

Typical examples of ionophores that have suffered from chemical instabilities are organotin compounds and ionophores with a UO_2 center. This is particularly unfortunate because both ionophore classes have shown very good phosphate selectivity, which is difficult to achieve since phosphate has a very high hydration energy and requires particularly strong and selective binding for the ionophore to permit preferential transfer of phosphate into the sensing membrane. Several UO_2-salophenes (e.g., **phosphate-I**) have shown interesting phosphate selectivity due to strong phosphate binding to the U(VI) center, but these ionophores may decompose in the presence of phosphate due to formation of inorganic uranium(VI) phosphate. Buffering of both phosphate and uranyl ions in the inner filling of the electrode is an interesting approach to extend the sensor life time.[130, 131] Ionophore decomposition was also observed for several organotin compounds. Very high phosphate selectivities could be achieved with an elegant design putting up to four Sn(IV) centers into one ionophore (**phosphate-II**),[132] but sensor lifetimes were limited to less than one day due to ionophore decomposition.

One approach that has been used to control stoichiometries is steric hindrance, as it is similarly discussed above for cation ionophores (Section 4.3). One of the nicest examples of this approach is the one of picket fence porphyrins.

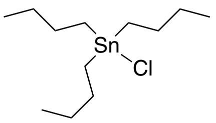

Cl^--II

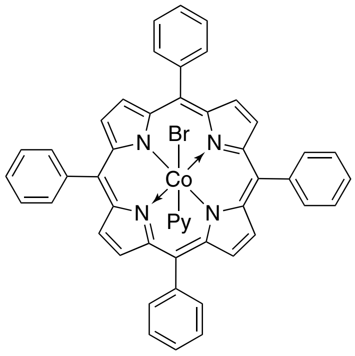

NO_2^--I

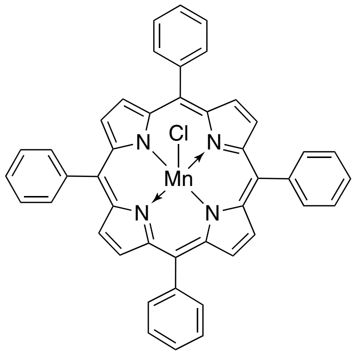

Cl^--III

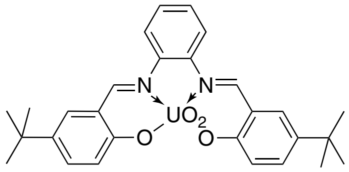

Phosphate-I

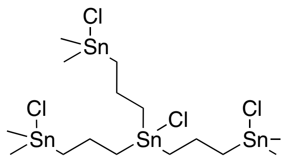

Phosphate-II

A common problem with metalloporphyrin-based ISEs is relatively high interference from OH^-. Indeed, OH^- binding to many metalloporphyrins is so strong that two metallophorphyrins may bind to one OH^- in a sandwichlike 2 : 1 complex.[129] A possible consequence of the high OH^- affinity is a rather complicated potentiometric response mechanism, as it is illustrated schematically in Figure 24. At high concentrations of the target anion X^- in the aqueous sample, the sensing membrane doped with a singly positively charged metalloporphyrin (as typical for metalloporphyrins with a M(III) metal center) and 33 mol% anionic sites contains ionophore complexes LX and free ionophore L^+ in a ratio 2 : 1 (Figure 24, left). Here, the ISE will respond to the target anion with the theoretical (Nernstian response) of −59 mV per 10-fold increase in the activity of X^- in the aqueous phase. When the ISE membrane is exposed to aqueous solutions of high pH and low X^- activity, ion exchange occurs, and the sensing membrane contains a 1 : 1 ratio of LOH and $[L_2OH]^+$ complexes (Figure 24, right). In this concentration range, the ISE does not respond to X^- but only to pH changes. At intermediate concentrations of X^- and OH^- in the sample (Figure 24, center), the sensing membrane contains a 1 : 1 ratio of LX and $[L_2OH]^+$. Because there is no free ionophore in this concentration range, the X^- concentration in the membrane is not buffered well, and unusual potentiometric responses such as apparently "twice-Nernstian" response of −116 mV per 10-fold increase in X^- at constant pH may be observed in this range.[49,122,129,133] This increase in response slope may appear attractive, but

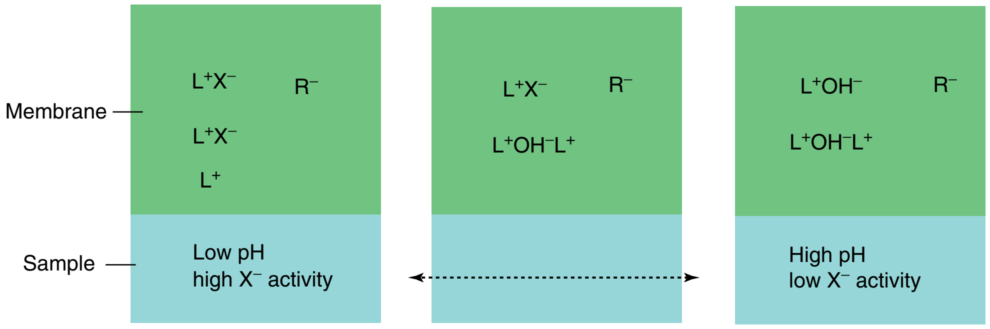

Figure 24 Formation of different ionophore complexes in an ionophore-doped membrane when exposed to sample solutions of differing hydroxide and target anion concentrations. Note the middle region in which target ion and hydroxide complexes of different stoichiometry coexist.

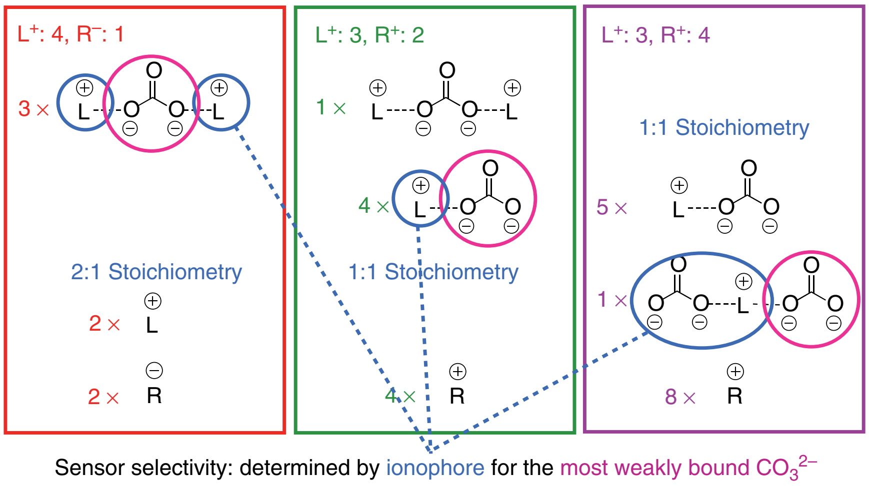

Figure 25 Formation of different CO_3^{2-} complexes of a positively charged ionophore (L^+) in membranes with different charges and concentrations of ionic sites.[114] Note that in membranes with more than one type of complexes, the potentiometric selectivity is determined by the most weakly bound ions.

unfortunately it is also accompanied by worse selectivities over other interfering ions than would be observed for ISEs with the left hand membrane composition.[133] Moreover, while response times of electrode membranes with compositions represented by the left hand side and center of Figure 24 are fast, the ion exchange that occurs in the transition range betweens these two regions causes very slow response times. This all points to the fact that simultaneous formation of LX and $[L_2OH]^+$ in an ISE membrane should be avoided. One very elegant approach to prevent the formation of $[L_2OH]^+$-type porphyrin complexes is to use porphyrins with very bulky peripheral substituents. Both In(III) and Ga(III) picket fence porphyrins have been successfully used in ISEs without observation of apparently "twice-Nernstian" responses (**picket fence porphyrin**).[129] Alternatively, dimer formation was avoided by attachment of the ionophore to the backbone of the polymer matrix.[64]

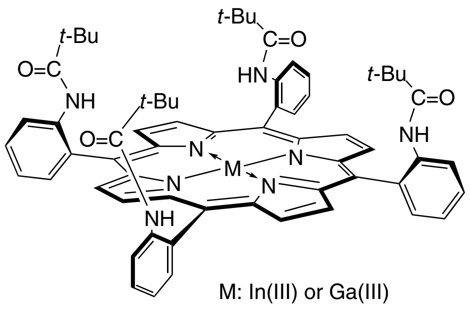

picket fence porphyrin

The apparently "twice-Nernstian" responses discussed above result from different complex stoichiometries for the target anion and OH^-. However, the target anion itself may also form complexes of different stoichiometries with the ionophore, an effect that can be controlled with the concentration and charge of the ionic sites. An example that was experimentally observed for a Mn(III) porphyrin is illustrated in Figure 25.[134] In this case, 25 mol% of anionic site relative to the ionophore result in the strongest binding of carbonate since two ionophores per carbonate assist the transfer of the carbonate into the sensing phase. When 67 mol% of cationic sites are used instead, a significant fraction of the carbonate in the membrane is only bound by one ionophore molecule, and when 133 mol% cationic sites are used, two carbonate molecules have to share one ionophore. The latter is possible because in a Mn(III) porphyrin axial ligands can bind to the Mn(III) center both from above and from below the porphyrin plane. Figure 26 shows the membrane composition for the same ionophore and ionic site ratios if the sensing membranes are exposed to solutions of the interfering ion thiocyanate. A whole different set of complexes is observed. Whether negatively or positively charged ionic sites give the higher selectivity, and which mole ratio of ionophore and ionic sites gives the most selective ISE membrane depends on the stoichiometries and stabilities of the complexes of the target anion and the interfering anions. Because these are typically not known in advance, different membrane compositions need to be tested experimentally to determine the most selective membrane compositions. While a thorough treatment is often not trivial, the amount of experimental work is somewhat reduced by the knowledge of specific ratios of ionic sites and ionophore that give the highest selectivities for specific complex stoichiometries and charges of ionophores, target ion, and interfering ions. The numerical values for the ratio of ionic sites and ionophore that

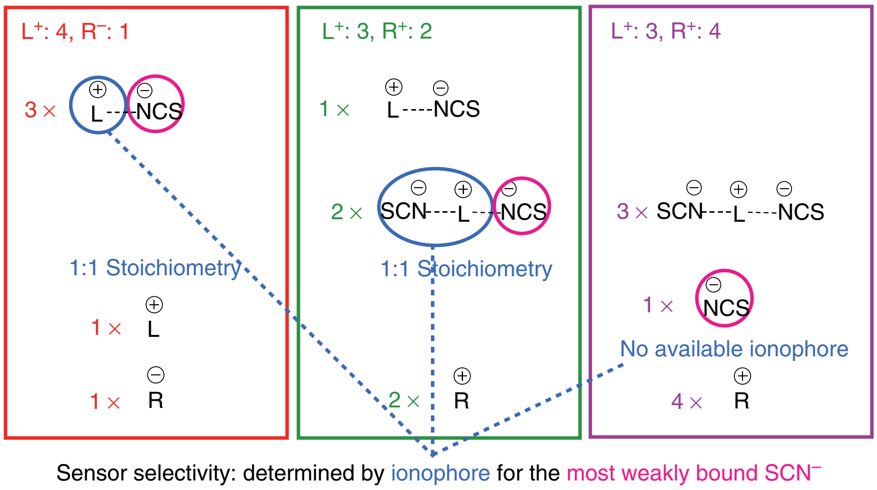

Figure 26 Formation of different SCN^- complexes of a positively charged ionophore (L^+) in membranes with different charges and concentrations of ionic sites.[114] SCN^- is chosen here as a representative interfering, and ionophore and site concentrations correspond to Figure 25.

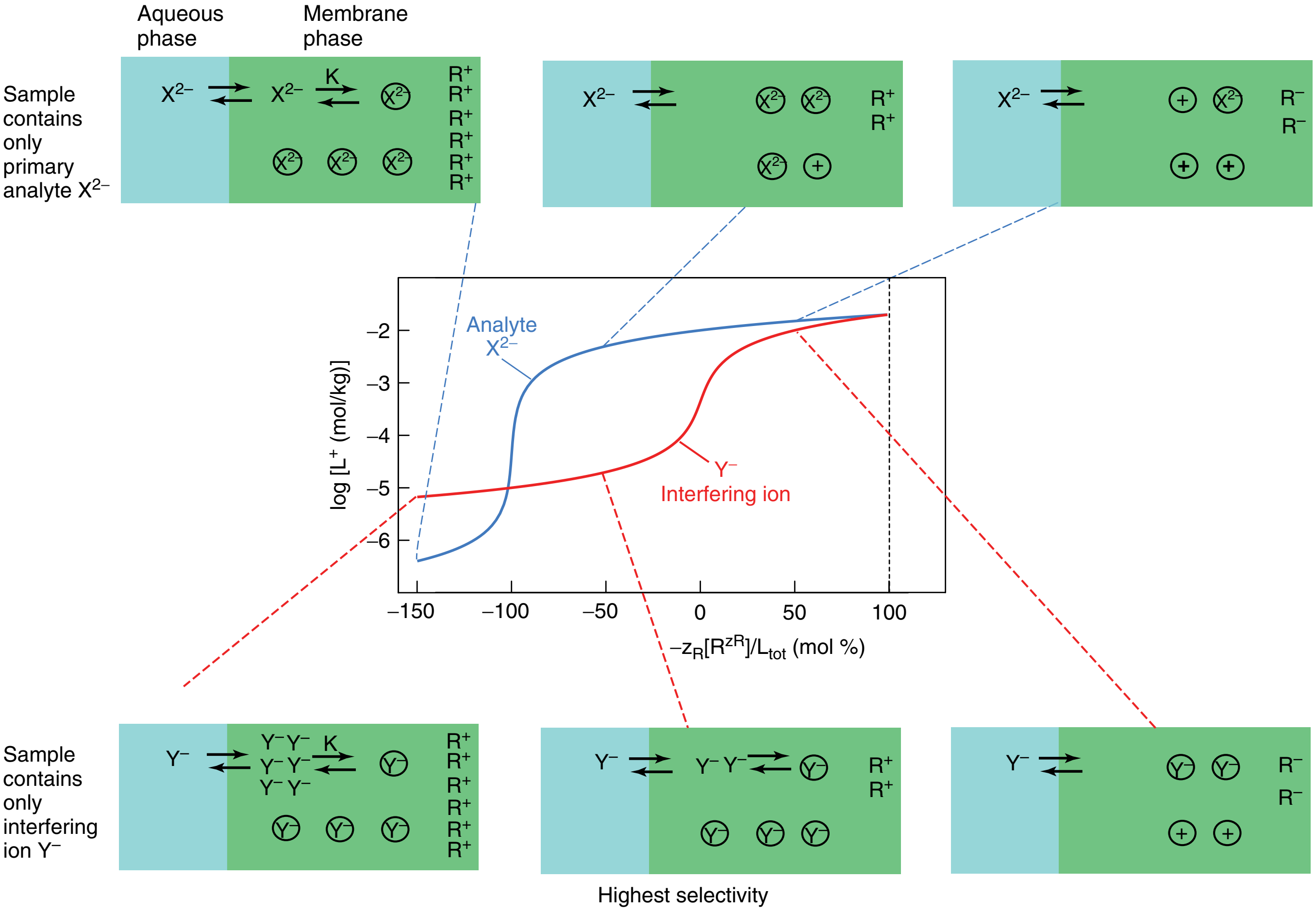

Figure 27 Dependence of the free ionophore concentration on the charge sign and concentration of ionic sites. Top row and blue line: divalent target ion. Bottom row and red line: monovalent interfering ion. The highest potentiometric selectivity is obtained at the ratio of ionic sites and ionophore for which there is a high concentration of free ionophore when the sensor is exposed to target ions but a very low concentration of free ionophore when the sensor is exposed to interfering ions.

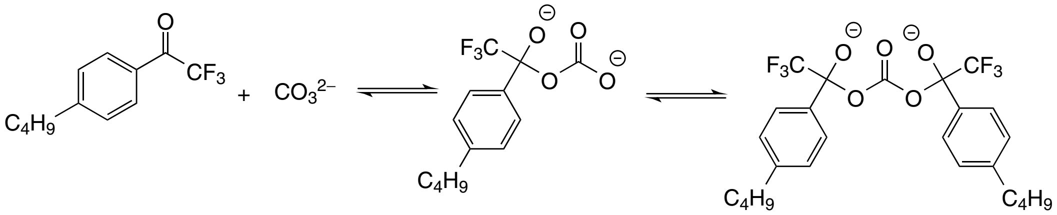

Figure 28 Covalent binding of $CO_3{}^{2-}$ to a trifluoroacetophenone ionophore.

give the highest selectivity are well known from theory and have been tabulated but typically cannot be predicted intuitively.[53,128,135,136] For example, for a singly positively charged ionophore L^+ that binds both the target anion X^{2-} and the interfering ion Y^- with 1 : 1 stoichiometry, the optimum ratio is 62 mol% cationic sites relative to the ionophore. Why this ratio provides the best selectivity is illustrated by Figure 27. It shows with a blue line how the concentration of free ionophore in the bulk of the sensing membrane exposed to an aqueous solution of primary anion X^{2-} depends on the concentration of the ionic sites in the sensing membrane. Note that positive values on the x-axis refer to cationic sites, and negative values to anionic sites. The red line gives the corresponding concentration of free ionophore in the sensing membrane if this membrane is exposed to solutions containing only the interfering anion Y^-. The optimum concentration of 62 mol% cationic sites corresponds to a membrane that has a high free ionophore concentration when the sensor is exposed to solutions of the target anion but a very low concentration of free ionophore when the membrane is exposed to interfering ions only (note the logarithmic scale of the y-axis). The same tabulated values for ionic site–ionophore ratios can also be used to investigate and optimize the selectivities of ISE membranes doped with electrically neutral ionophores, but note that for those ionophores this selectivity optimization is often simpler because the number of conceivable complexes is often smaller.[53,128,135,136]

4.6 Ionophores that form covalent bonds to the target ion

Only a small number of ISEs based on an ionophore that binds the analyte of interest by formation of a covalent bond have been reported. Many of them are carbonate-selective electrodes, which are of great interest to clinical chemistry and environmental monitoring. Initially introduced as inert membrane matrixes, trifluoroacetyl-p-alkylbenzenes were found to give ISEs a good selectivity for carbonate. Further studies confirmed that carbonate binds to trifluoroacetophenone derivatives by nucleophilic addition to the carbonyl group,[137] resulting in the formation of a covalent bond (Figure 28).[138–142] However, because the concentration of $CO_3{}^{2-}$ at physiological pH is low in comparison to that of $CO_3{}^{2-}$, these ISEs suffered from interference of ions such as Cl^-, Br^-, and salicylate. The latter two are not typically present in the human body, but are components of common drugs. Therefore, significant effort has been spent to prepare improved carbonate-selective electrodes. Most of this work has been devoted to the development of trifluoroacetophenone derivatives with different substituents on the aromatic ring. Replacing of alkyl substituent in para position by electron acceptors such as amide, ester, and sulfone groups or adding strong electron withdrawing groups, such as NO_2 or Br, in meta position enhanced selectivities by up to 1.5 orders of magnitude.[143–145] Moreover, a neighboring group that stabilizes the carbonate–ionophore complex through intramolecular H bonding resulted in a more than 10-fold enhancement in CO_3^{2-} selectivity.[146] Also, molecular tweezers-type ionophores have been also obtained by coupling two trifluoroacetobenzoyl groups in one receptor, providing 10- to 300-fold improved selectivity for $CO_3{}^{2-}$ over other anions.[147]

Because the carbonate selectivity provided by these ionophores is often not satisfactory enough, supplementary approaches have been used to reduce interference from highly lipophilic anions, such as salicylate and perchlorate. These include coating of the ionophore-doped sensing membrane with a hydrophilic, porous layers that slows down the access of large, lipophilic anions such as salicylate to the sensing membrane.[148–151]

A similar concept as for carbonate ionophores has also been used for sulfite sensors. In this case, the well-known addition of sulfite to benzaldehyde derivatives by reversible formation of a covalent bond has been taken advantage of (Figure 29).[152] However, while used for ion-selective optodes, this approach has not been tested for ISEs. Optodes based on the addition of H_2O or alcohols to phenyl ketones have also been reported for the detection of humidity and alcohols in beverages, respectively, but because of the nonionic nature of these analytes, ISEs based on these ionophores are not feasible.[4]

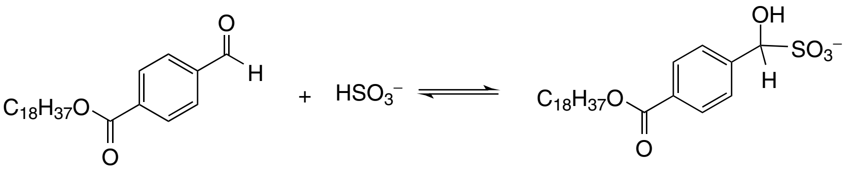

Figure 29 Covalent binding of HSO_3^- to a benzaldehyde ionophore.

4.7 Ionophore-based ion-selective electrodes for organic ions

One approach to the detection of electrically neutral organic analytes is based on the use of enzymes that catalyze the formation of an ion that can be detected potentiometrically, as discussed in Section 3.1.7. The direct detection of electrically neutral organic species with ISEs is not possible since the transfer of these species across the interface of an aqueous sample into an ISE membrane does not involve the transfer of an electric charge across this interface. However, electrically neutral species can affect the phase boundary potential indirectly. Several studies have shown how alcohols, carboxylic acids, and oligoethers (including several surfactants of this type) cause a potentiometric response upon distribution from the aqueous sample into ionophore-free cation-exchanger membranes loaded with metal cations.[4,153,154] This can be explained by specific binding of these electrically neutral, hydrophobic organic species in the ISE membrane to the metal cations, which lowers the activity of the metal cation in the sensing membrane and causes a change in the phase boundary potential at the sample–membrane interface (2). An analogous principle has also been described for the detection of phenols.[155] While this approach does not involve the use of an ionophore, the interaction of the metal cation with these organic substrates falls undoubtedly within the field of host–guest chemistry.

A much larger number of ISEs have been proposed for the detection of electrically charged organic analytes. Many of these ISEs fall into the category of ionophore-free ion-exchanger electrodes, and while they do often exhibit high selectivities for fairly hydrophobic organic ions over many inorganic ions, they are from the point of view of supramolecular chemistry not of interest. However, a number of ionophores have been used to prepare ISEs for the detection of organic ions. Some of these ionophores have structures that are quite similar to those of ionophores used in ISEs for inorganic ions. These include, for example, crown ethers and calixarenes used for the detection of protonated amines and amino acid esters, and metalloporphyrins for the detection of anions.[4] Recent examples include, for example, tin(IV) and zirconium (IV) porphyrins for the monotopic recognition of phthalate (**phthalate**)[156] and citrate (**citrate**),[157] respectively.

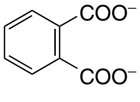

Phthalate

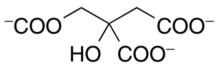

Citrate

Other ionophores have been specifically designed for the selective recognition of organic analytes. Among the recent particularly unique examples are receptors with three trifluoroacetophenone groups for the recognition of phenylalanine (**phenylalanine-I**)[158] and sophisticated hydrogen-bonding hosts for nucleobases, such as the adenosine 5′-monophosphate binding receptor **AMP-I**.[159]

A special feature of organic ions is that many of them are optically active. Since the complexes of a chiral ionophore with two enantiomers are diastereomers, their formation energies differ from one another and permit the preparation of enantioselective ISEs. While already recognized back in the 1970s,[4] examples for this concept continue to be reported on a regular basis. The organic chemist will recognize in ionophores used for this purpose structural elements familiar from enantioselective catalysis. A typical recent example is the popular binaphthyl group of **phenylglycineOCH$_3$-I**, a receptor that has been used for the enantioselective potentiometric detection of phenylglycine methyl ester.[160]

In summary, considerable efforts have been spent to show the feasibility of ISEs for organic analytes. While some authors used ionophore-based ISEs to measure organic target analytes in relatively simple samples such as drug tablets that contained besides the analyte only hydrophilic inorganic ions, only very few reports exist on the use of such electrodes for measurements in more complex samples such as blood, saliva, or milk.

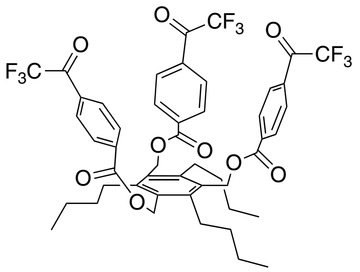

Phenylalanine-I

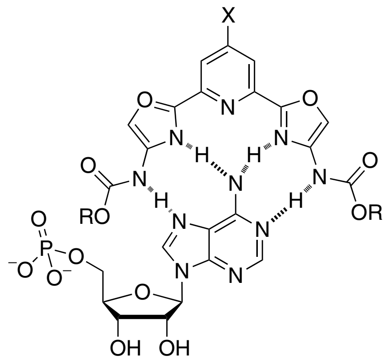

AMP-I

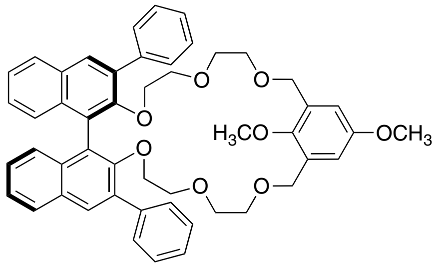

PhenylglycineOCH$_3$-I

5 QUANTITATIVE THEORY OF ION-SELECTIVE ELECTRODES THAT BENEFITS THE HOST–GUEST CHEMIST

5.1 Quantification of selectivity

Selectivity is not only a main characteristic of an ISE, but it can also be used to determine the stoichiometries and stabilities of ionophore complexes and to optimize the selectivity in view of specific applications (Section 4.3). In extension of the Nernst equation (1), the potentiometric selectivity coefficient, $K_{i,j}^{\text{pot}}$, is given by the following equation[3,50,136,161]:

$$\text{EMF} = E^{\circ} + \frac{2.303RT}{z_i F} \log\left(a_i + K_{i,j}^{\text{pot}} a_j^{z_i/z_j}\right) \qquad (7)$$

where a_{i} is the concentration of the ion of interest—often referred to as the primary ion—and a_j is the concentration of an ion j potentially interfering with the determination of ion i. In the absence of interfering ions, (7) simplifies to the Nernst equation (1). In the absence of primary ions, (7) simplifies to the Nernstian equation formulated for the interfering ion j, but with a different intercept (i.e., $E^{\circ\prime}$).

$$\begin{aligned}\text{EMF} &= E^{\circ} + \frac{2.303RT}{z_i F} \log\left(K_{i,j}^{\text{pot}} a_j^{z_i/z_j}\right) \\ &= E^{\circ} + \frac{2.303RT}{z_i F} \log(K_{i,j}^{\text{pot}}) + \frac{2.303RT}{z_j F} \log a_j \\ &= E^{\circ\prime} + \frac{2.303RT}{z_j F} \log a_j \qquad (8)\end{aligned}$$

The different value for the intercept reflects the different free energies of transfer of the primary and interfering ions from the aqueous sample into the ISE membrane and the different free energies of complexation.

Equation (8) correctly predicts the different response slope of the calibration curve for an interfering ion that differs in the charge number from the primary ion. Moreover, when the primary and interfering ion have the same charge number and the two ions form complexes of the same stoichiometry, (7) not only predicts the response of an ISE to solution of ions i or j, but it also applies to mixed solutions of the two ions. An example for a response to the primary ion i with a constant background concentration of ion j is shown in Figure 30. At low concentrations the ISE responds only to the interfering ions, and at high concentrations the ISE responds only to the

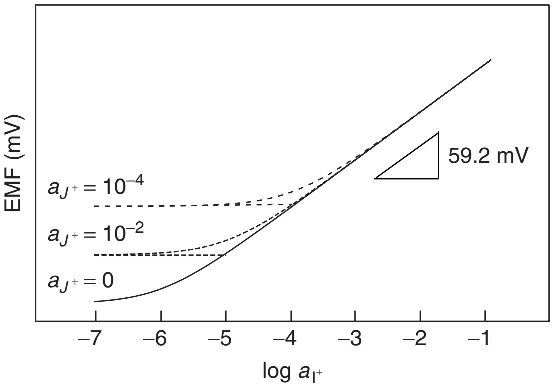

Figure 30 Potentiometric responses to a primary ion (I^+) in a background with a constant concentration of an interfering ion (J^+). Note that the lower detection limit for the primary ion worsens as the concentration of the interfering ion increases.

primary ion. The crossing point obtained from the extrapolation of the two linear sections of the response curve can be used to determine $K_{i,j}^{\mathrm{pot}}$. This method of selectivity determination is referred to as the fixed interference method (FIM),[136,161] while the complementary method of measuring the response to the interfering ion in a fixed background of primary ion is referred to as fixed primary ion method (FPIM). When the primary and interfering ions have different charges or form complexes of different stoichiometries, the potentiometric response in a relatively narrow region near the crossing point of the linear response sections differs slightly from what is predicted by (7). These effects have been discussed elsewhere[50,162] and are beyond the scope of this chapter, in particular, since even in those cases the extrapolation of the linear sections can still be used to determine $K_{i,j}^{\mathrm{pot}}$ values. A different approach for the determination of $K_{i,j}^{\mathrm{pot}}$ values is the separate solution method (SSM),[136,161] which is based on the measurement of the calibration curves for separate solutions that contain either only primary ions or only interfering ions (Figure 31). If they are carefully performed, the FIM, FPIM, and SSM methods all give within error the same values for $K_{i,j}^{\mathrm{pot}}$. This requires most importantly that only sections of the EMF response curve in which the ISE exhibits a Nernstian response to the primary or interfering ion are used. When experiments are performed carefully, differences in $\log K_{i,j}^{\mathrm{pot}}$ experimentally determined with different methods do not exceed 0.1–0.2 units, and larger differences are cause of concern.

Evidently, an interfering ion characterized by a very small value of $K_{i,j}^{\mathrm{pot}}$ affects the measured EMF only at very low activities of the primary ion. On the other hand, strongly interfering ions have very large values of $K_{i,j}^{\mathrm{pot}}$. There are no generally acceptable or unsatisfactory $K_{i,j}^{\mathrm{pot}}$ values. What value of $K_{i,j}^{\mathrm{pot}}$ can be tolerated depends on the specific application for which the ISE is used. For example, when Na^+ with an expected activity in the 140 mM range is measured in blood with an expected H^+ activity around $10^{-7.2}$ M (i.e., pH 7.2), $K_{\mathrm{Na,H}}^{\mathrm{pot}}$ value can be relatively high without a cause of concern. On the other hand, a pH measurement in the same sample requires a very small value of $K_{\mathrm{H,Na}}^{\mathrm{pot}}$ since the H^+ activity is more than six orders of magnitude lower than the Na^+ activity.

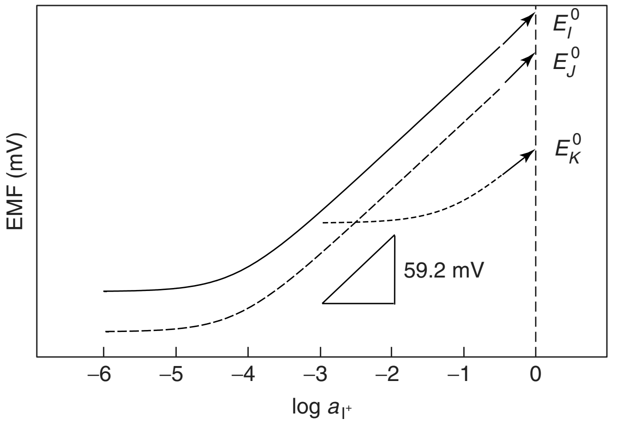

Figure 31 Potentiometric response curves to the primary and interfering ions as measured with the separate solution method (SSM). As illustrated for ion K, the detection limit of the ISE may be significantly worse than for the primary ion and may make it difficult to determine unbiased selectivity coefficients.

The best ISEs developed over recent years are characterized by $K_{i,j}^{\mathrm{pot}}$ values for different ions that cover many orders of magnitude. As a result, selectivity coefficients are typically reported for convenience on a logarithmic scale as $\log K_{i,j}^{\mathrm{pot}}$ values, which is also more informative when presented graphically. This approach distinguishes ISE publications from many reports on chemical sensing in the general, organic, and biological chemistry literature, where changes in an observed variable such as absorbance or fluorescence are not infrequently reported for an arbitrary concentration. For example, some authors may have observed the formation of a fluorescent complex between Ag^+ and a new silver ionophore and measured the fluorescence intensity at a silver concentration of 10^{-6} M. They then proceed to measure the fluorescence intensity for 10^{-6} M solutions of other metal ions and report the fluorescence intensity for those ions in percent relative to the fluorescence intensity for Ag^+. Clearly, values such as <5% or 25% give an excellent first snapshot of the overall selectivity of a new sensing probe, but such data have limited predictive power for what will be observed at different concentrations. This makes it quite difficult to compare different probes reported by different authors. In comparison, there is a significant advantage to having a specific value of $\log K_{i,j}^{\mathrm{pot}}$ that can be used to assess possible interference (or lack thereof) for wide ranges of primary and interfering ion concentrations and concentration ratios. As an analytical chemist, one wishes that this concept were more widely applied by other researchers interested in the development of sensing probes. This shall not mean though that this concept is unique to ISEs. Indeed, there are analogies in concepts as far as, for example, toxicology, where the dose of a compound that affects 50% of test animals lethally is defined as LD50. Evidently, it would not make sense to characterize drugs by their effect at one arbitrary dose at which the effect of weakly toxic compounds is not detected at all and a moderately toxic compound cannot be distinguished from a highly toxic one because they both result in 100% lethality.

5.2 Effect of the ionophore–ionic site ratio on selectivity and determination of complex stoichiometries and binding constants

In Sections 3.1.2 and 4.4, it was already pointed out that the ratio of ionophore and ionic sites has a profound effect on the potentiometric selectivity. Without going into much detail, this effect will be discussed here from an intuitive point of view and under special consideration of the complex stoichiometry. Moreover, this section will emphasize how the stability of complexes formed in ISE membranes can be determined experimentally.

Consider, for example, a very simple electrically neutral Ag^+ ionophore with one thioether group that is suspected to form the complexes LAg^+, L_2Ag^+, L_3Ag^+, and L_4Ag^+. The best approach to confirm this stoichiometry is to prepare ISE membranes that contain the ionophore and hydrophobic anionic sites in different ratios and measure the selectivity over an interfering ion that can be reasonably assumed not to bind to the ionophore at all. Often, tetrabutylammonium and tetraphenylphosphonium are good candidates for noninteracting ions.[67,163] What changes in selectivity would one expect when the molar ratio of ionophore and ionic sites is changed in several steps from 0 to 6? (Most of the literature refers to site-to-ionophore ratios, but in this example the inverse of that value is used since this simplifies the discussion here.) Figure 32 shows selectivities calculated based on well established theory[3,45] for an ionophore that forms only 1 : 1 complexes (curve b), 1 : 1 and 2 : 1 complexes (c), 1 : 1, 2 : 1, and 3 : 1 complexes (d), and 1 : 1, 2 : 1, 3 : 1, and 4 : 1 complexes (e). At the 0.5 : 1 ratio, at least half of the Ag^+ in all four membranes occurs in the form of free Ag^+ not bound to an ionophore. The unbound Ag^+ dominates the selectivity, and the ISE selectivity differs little from the one for an ionophore-free ion-exchanger membrane (no ionophore, only anionic sites). At the 5 : 1 ratio of ionophore to ionic sites, the selectivity for Ag^+ increases (i.e., the selectivity coefficient decreases) from (b) to (c), (d), and (e), as it is expected for the increasing maximum complex stoichiometries. As the ratio of total ionophore to ionic sites increases from 0 to 5, there is for every case one very distinct $[L_{tot}]/[R^-]$ value at which the selectivity changes quite suddenly. This value equals for all four calculated cases the number of ionophore molecules per Ag^+ ion in the respective complex of the highest possible stoichiometry. Consequently, an experimental variation of the $[L_{tot}]/[R^-]$ ratio can be used to determine the stoichiometry of ionophore complexes.

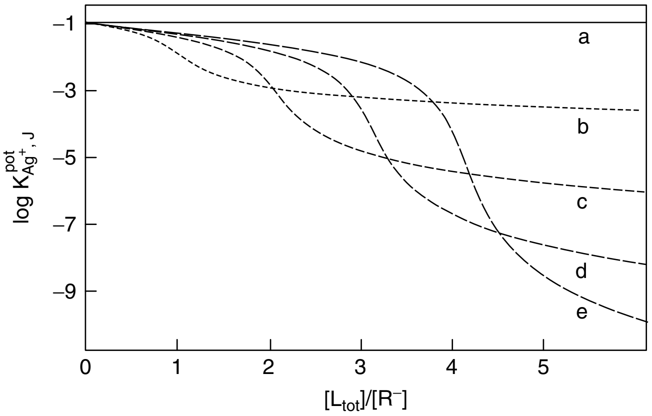

Figure 32 Selectivity of an ISE for Ag^+ over an interfering ion (J^+) that does not bind to an electrically neutral ionophore: Effect of the molar ratio of the total ionophore concentration to anionic sites. The five different curves show the dependence of the selectivity as calculated for ionophores that form complexes of different stoichiometries: (a) ionophore does not bind Ag^+ at all; (b) $\beta_{AgL} = 10^5$; (c) $\beta_{AgL} = 10^5$, $\beta_{AgL2} = 10^{10}$; (d) $\beta_{AgL} = 10^5$, $\beta_{AgL2} = 10^{10}$, $\beta_{AgL3} = 10^{15}$; (e) $\beta_{AgL} = 10^5$, $\beta_{AgL2} = 10^{10}$, $\beta_{AgL3} = 10^{15}$, $\beta_{AgL4} = 10^{20}$, where the cumulative complex stabilities are defined as $\beta_{AgLn} = [AgL_n]/([Ag^+][L]^n)$. The selectivity at $[L_{tot}]/[R^-] = 0$ reflects the different energies of phase transfer from the aqueous into the ionophore-free membrane phase for Ag^+ and J^+. Calculated for $K_{ex,Ag/J} = 0.1$, $[R^-] = 1$ mM. For this calculation, it was assumed that the cumulative binding constants increase from 1 : 1 to 4 : 1 in increments of 10^5, which is equivalent to assuming that all ligands in all complexes bind to the metal center equally strong.

It is noteworthy that the calculated selectivity curves intersect with one another, which might not be expected intuitively. To explain this, consider the 1.5 : 1 ratio. On one hand, approximately half of the Ag^+ is in the form of L_2Ag^+ complexes if the ionophore can form such a complex, and the free ionophore concentration and potentiometric selectivity are low. On the other hand, one-third of the ionophore is in its free form if only 1 : 1 complexes can form, and as a result of the relatively high free ionophore concentration the selectivity is high. The direct consequence is that for each curve (i.e., each set of binding constants) there are not multiple but there is

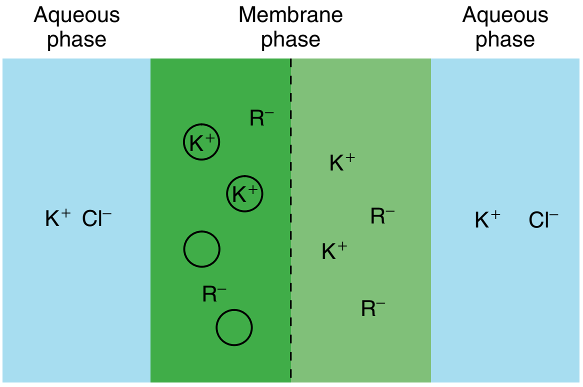

Figure 33 Determination of the stability of ionophore complexes with the sandwich membrane method: Only the left hand membrane contains ionophore.

only one single step in selectivity. For example, curve (e) exhibits only one step and not a step each at $[L_{tot}]/[R^-]$ values of 1, 2, 3, and 4. Therefore, the observation of one step only should not be misinterpreted as an indication that only one type of complex can be formed. In every case, an increase of the ionophore-site ratio well beyond the maximum stoichiometry causes only small additional increases in selectivity because the complex stoichiometry does not change further, and the increase in free ionophore is only moderate.

One approach to determine binding constants is to quantitatively compare the difference in potentiometric selectivity for an ion of interest (versus an noninteracting ion) at $[L_{tot}]/[R^-] = 0$ and at a $[L_{tot}]/[R^-]$ value for which the membrane contains free ionophore.[163] An alternative approach to determine binding constants and a method to test whether the presumably noninteracting interfering ion really does not bind to the ionophore is the so-called sandwich membrane technique (Figure 33).[164,165] Using this technique, two membranes are prepared in first place. One of them contains only ionic sites, and the other one contains ionophore and the ionic sites in the desired ratio. Both membranes are equilibrated with aqueous solutions of the primary ion. The ionophore-doped membrane is then mounted into a conventional electrode body with an internal reference, and the potentiometric response, $E_{\text{ionophore}}$, relative to an external reference electrode is measured. Subsequently, the ionophore-doped membrane is dismounted, the ionophore-free membrane is pressed onto the ionophore-doped membrane, and the thus obtained membrane sandwich is quickly mounted into the electrode body and the potential is remeasured to give E_{sandwich}. Subtraction of E_{sandwich} from $E_{\text{ionophore}}$ eliminates all the contributions from the internal reference and the external reference electrode as well as the phase boundary potential at the interface of the ionophore-doped segment and the aqueous sample. The difference between E_{sandwich} and $E_{\text{ionophore}}$ equals the sum of the three phase boundary potentials at the interfaces of the aqueous sample and the ionophore-doped membrane, the ionophore-doped membrane and the ionophore-free membrane, and the ionophore-free membrane and the aqueous sample. However, the two membrane segments are made of the sample material and form between them an interface between two miscible solutions for which it has been shown that the liquid junction potential, E_{ll}, is very small.[166] Assuming that $E_{\text{ll}} \approx 0$ V and flipping a sign, $E_{\text{sandwich}} - E_{\text{ionophore}}$ is calculated to be the difference of the two-phase boundary potentials at the interface of the aqueous sample and the ionophore-doped membrane on one hand, and the interface of the aqueous sample and the ionophore-free membrane on the other hand. E_{sandwich} differs from $E_{\text{ionophore}}$ because the concentration of the free primary ion in the ionophore-free segment equals the concentration of ionic sites, while the concentration of the free primary ion in the ionophore-doped segment is much lower because it is buffered by the free ionophore and ionophore complex. Indeed, multiplication of $E_{\text{sandwich}} - E_{\text{ionophore}}$ with $-z_i F/RT$ and raising Euler's number to the power of the resulting term gives the concentration ratio of the free primary ion in the ionophore-doped and ionophore-free membrane segments, from which the binding constant can be calculated using the known ionophore and complex concentrations. Evidently, in the case of an ion that does not bind to the ionophore, $E_{\text{sandwich}} - E_{\text{ionophore}}$ has to be 0 V.

6 CONCLUSIONS

A discussion of the state of the art of ISEs for every target ion for which such sensors have been developed would have been well beyond the scope of this chapter. However, we hope that this chapter gives the interested reader an overview of state-of-the-art ionophore-based potentiometry that goes beyond a superficial treatment and illustrates what developers of ISEs need to consider when they want to take advantage of host–guest chemistry to fabricate highly selective sensors. As some of the examples show, analytical chemists have developed a variety of techniques for the optimization of ionophore-doped membranes. This has led to sensors with remarkably high selectivities and extraordinarily low detection limits.

Evidently, the field of ISEs has become very sophisticated and a lot of ionophore design has been performed, both by analytical chemists and organic chemists. This raises the question where the future of ISEs is heading. What are the needs for analysis with ISEs in real-life situations? It seems quite clear that many analytical chemists will continue to focus on the development of new approaches to further lower detection limits, improve sensor life time and robustness, reduce the frequency of calibration, and find new applications for ISEs. However, since ionophores are the key to the high selectivities of ISEs, it is clear that the development of new ionophores will remain an activity central to ion-selective potentiometry. For a small number of ions the available ionophores are selective enough for all but very few applications. This seems to be true, for example, for H^+, Na^+, K^+, Ca^{2+}, and Ag^+. However, this list is short, and many cations are missing from it. For example, more selective Mg^{2+} and NH_4^+ ionophores would be useful for a variety of practical applications. Moreover, anions are conspicuously absent from this list. For example, more selective ISEs for the strongly hydrophilic phosphate and sulfate are still much in need, and could have a strong impact on clinical, biochemical, process and environmental analysis. Even for chloride reliable, more selective sensors for clinical analysis would be highly desirable. While arrays of sensors with low selectivity ("electronic tongues" and "electronic noses")[167] can serve a purpose when samples contain a limited number of well-known compounds in a limited range of concentrations, it has become clear that highly selective sensors are always preferred for measurements with high accuracy and precision.

The need for better ionophores will make sure that the work of those who practice host–guest chemistry will continue to be much valued in ion-selective potentiometry. Care must, however, be taken to ensure that reported selectivities are reproducible and accurately reflect the thermodynamics of complex stoichiometries and complex stabilities.[136,161] There is an ever increasing number of reports on ISEs based on new ionophores, but not all reported work reflects on the full complexity and potential of the often hard to synthesize ionophores. It is the hope of the authors that this chapter has contributed to span the gap between on one hand (too) simple introductions to ISEs and, on the other hand, the intimidating plethora of recent publications written for the specialist.

REFERENCES

1. W. E. Morf, *The Principles of Ion-Selective Electrodes and of Membrane Transport*, Elsevier, New York, 1981.
2. D. Ammann, P. Anker, P. C. Meier, *et al*., *Ion Sel. Electrode R.*, 1983, **5**, 3–92.
3. E. Bakker, P. Bühlmann, and E. Pretsch, *Chem. Rev.*, 1997, **97**, 3083–3132.
4. P. Bühlmann, E. Pretsch, and E. Bakker, *Chem. Rev.*, 1998, **98**, 1593–1687.
5. E. Lindner and R. P. Buck, *Anal. Chem.*, 2000, **72**, 336A–345A.
6. E. Bakker and E. Pretsch, *Anal. Chem.*, 2002, **74**, 420A–426A.
7. J. Bobacka, A. Ivaska, and A. Lewenstam, *Chem. Rev.*, 2008, **108**, 329–351.
8. E. Bakker and E. Pretsch, *Trends Anal. Chem.*, 2001, **20**, 11–19.
9. T. Sokalski, A. Ceresa, T. Zwickl, and E. Pretsch, *J. Am. Chem. Soc.*, 1997, **119**, 11347.
10. T. Sokalski, A. Ceresa, M. Fibbioli, *et al*., *Anal. Chem.*, 1999, **71**, 1210–1214.
11. A. Ceresa, E. Bakker, B. Hattendorf, *et al*., *Anal. Chem.*, 2001, **73**, 343–351.
12. J. Sutter, A. Radu, S. Peper, *et al*., *Anal. Chim. Acta*, 2004, **523**, 53–59.
13. A. Michalska, J. Dumanska, and K. Maksymiuk, *Anal. Chem.*, 2003, **75**, 4964–4974.
14. W. Qin, T. Zwickl, and E. Pretsch, *Anal. Chem.*, 2000, **72**, 3236–3240.
15. A. Malon, T. Vigassy, E. Bakker, and E. Pretsch, *J. Am. Chem. Soc.*, 2006, **128**, 8154–8155.
16. C. Z. Lai, M. A. Fierke, R. C. da Costa, *et al*., *Anal. Chem.*, 2010, **82**, 7634–7640.
17. E. Bakker, *J. Electrochem. Soc.*, 1996, **143**, L83–L85.
18. M. J. Berrocal, R. D. Johnson, I. H. A. Badr, *et al*., *Anal. Chem.*, 2002, **74**, 3644–3648.
19. M. C. Frost, M. M. Reynolds, and M. E. Meyerhoff, *Biomaterials*, 2005, **26**, 1685–1693.
20. Y. D. Wu and M. E. Meyerhoff, *Talanta*, 2008, **75**, 642–650.
21. A. E. Martell and R. J. Motekaitis, *Coord. Chem. Rev.*, 1990, **199**, 323–361.
22. K. A. Connors, *Binding Constants*, John Wiley & Sons, Ltd, New York, 1987.
23. M. Dole, *J. Chem. Educ.*, 1980, **57**, 134.
24. W. G. Hines and R. de Levie, *J. Chem. Educ.*, 2010, **87**, 1143–1153.
25. C. Moore and B. C. Pressmann, *Biochem. Biophys. Res. Commun.*, 1964, **15**, 562.
26. Z. Stefanac and W. Simon, *Chimia*, 1966, **20**, 436.
27. M. S. Frant, *J. Chem. Educ.*, 1997, **74**, 159–166.
28. H.-K. Wipf, L. A. R. Pioda, Z. Stefanac, and W. Simon, *Helv. Chim. Acta*, 1968, **51**, 377–381.
29. W. Simon, U. Spichiger, D. Freiner, *et al*. *Bull. Eidg. Techn. Hochschule Zürich*, 1991, Nr. **236**, 14.
30. P. C. Gunaratna, W. F. Koch, R. C. Paule, *et al*., *Clin. Chem.*, 1992, **38**, 1459–1465.
31. R. A. Steiner, M. Oehme, D. Ammann, and W. Simon, *Anal. Chem.*, 1979, **51**, 351–351.
32. T. J. Rink, R. Y. Tsien, and A. E. Warner, *Nature*, 1980, **283**, 658–660.
33. D. Ammann *Ion-Selective Microelectrodes*, Springer-Verlag, Berlin, 1986.
34. A. Radomska, E. Bodenszac, S. Glab, and R. Koncki, *Talanta*, 2004, **64**, 603–608.
35. R. W. Cattrall and I. C. Hamilton, *Sel. Electrode. Rev.*, 1984, **6**, 125–172.

36. A. Cadogan, Z. Gao, A. Lewenstam, *et al*., *Anal. Chem.*, 1992, **64**, 2496–2501.
37. G. A. Crespo, S. Macho, and F. X. Rius, *Anal. Chem.*, 2008, **80**, 1316–1322.
38. C.-Z. Lai, M. A. Fierke, A. Stein, and P. Bühlmann, *Anal. Chem.*, 2007, **79**, 4621–4626.
39. J. Koryta, *Electrochim. Acta*, 1979, **24**, 293.
40. Y. Shao, M. D. Osborne, and H. H. Girault, *J. Electroanal. Chem.*, 1991, **318**, 101–109.
41. S. Makarychev-Mikhailov, A. Shvarev, and E. Bakker, *J. Am. Chem. Soc.*, 2004, **126**, 10548–10549.
42. A. Shvarev and E. Bakker, *Anal. Chem.*, 2003, **75**, 4541–4550.
43. M. Kasuno, Y. Kakitani, Y. Shibafuji, *et al*., *Electroanal.*, 2009, **21**, 2022–2029.
44. V. Bhakthavatsalam and E. Bakker, *Electroanal.*, 2008, **20**, 225–232.
45. E. Bakker, P. Bühlmann, and E. Pretsch, *Talanta*, 2004, **63**, 3–20.
46. Y. Marcus, *Biophys. Chem.*, 1994, **51**, 111–127.
47. K. Tohda, Y. Umezawa, S. Yoshiyagawa, *et al*., *Anal. Chem.*, 1995, **67**, 570–577.
48. H. H. J. Girault and D. J. Schiffrin, *Electroanalytical Chemistry*, eds. A. J. Bard, Marcel Dekker, New York, 1989, vol. 15, pp. 1.
49. S. Amemiya, P. Bühlmann, and Y. Umezawa, *Anal. Chem.*, 1998, **70**, 445–454.
50. M. Nagele, E. Bakker, and E. Pretsch, *Anal. Chem.*, 1999, **71**, 1041–1048.
51. P. Bühlmann, S. Yajima, K. Tohda, and Y. Umezawa, *Electrochim. Acta*, 1995, **40**, 3021–3027.
52. P. Bühlmann, S. Amemiya, S. Yajima, and Y. Umezawa, *Anal. Chem.*, 1998, **70**, 4291–4303.
53. S. Amemiya, P. Bühlmann, E. Pretsch, *et al*., *Anal. Chem.*, 2000, **72**, 1618–1631.
54. R. Dohner, D. Wegmann, W. E. Morf, and W. Simon, *Anal. Chem.*, 1986, **58**, 2585.
55. E. Lindner, K. Toth, and E. Pungor, *Dynamic Characteristics of Ion-Selective Electrodes*, CRC Press, Boca Raton, 1988.
56. P. Bühlmann, M. Hayakawa, T. Ohshiro, *et al*., *Anal. Chem.*, 2001, **73**, 3199–3205.
57. G. J. Moody, R. B. Oke, and J. D. R. Thomas, *Analyst*, 1970, **95**, 910.
58. G. J. Moody, B. B. Saad, and J. D. R. Thomas, *Sel. Electrode Rev.*, 1988, **10**, 71–106.
59. R. D. Armstrong and G. Horvai, *Electrochim. Acta*, 1990, **35**, 1–7.
60. R. Eugster, T. Rosatzin, B. Rusterholz, *et al*., *Anal. Chim. Acta*, 1994, **289**, 1–13.
61. E. C. Lugert, T. P. Lodge, and P. Bühlmann, *J. Polym. Sci., Part B: Polym. Phys.*, 2008, **46**, 516–525.
62. C.-Z. Lai, S. S. Koseoglu, E. C. Lugert, *et al*., *J. Am. Chem. Soc.*, 2009, **131**, 1598–1606.
63. K. N. Phillips, C. Lantz, and P. Bühlmann, *Electroanal.*, 2005, **17**, 2019–2025.
64. Y. Qin and E. Bakker, *Anal. Chem.*, 2004, **76**, 4379–4386.
65. P. G. Boswell, E. C. Lugert, J. Rabai, *et al*., *J. Am. Chem. Soc.*, 2005, **127**, 16976–16984.
66. P. G. Boswell and P. Bühlmann, *J. Am. Chem. Soc.*, 2005, **127**, 8958–8959.
67. P. G. Boswell, C. Szijjarto, M. Jurisch, *et al*., *Anal. Chem.*, 2008, **80**, 2084–2090.
68. S. D. Moss, J. Janata, and C. C. Johnson, *Anal. Chem.*, 1975, **47**, 2238–2243.
69. B. A. McKinley, *Chem. Rev.*, 2008, **108**, 826–844.
70. J. Bobacka, A. Ivaska, and A. Lewenstam, *Electroanal.*, 2003, **15**, 366–374.
71. M. A. Fierke, C.-Z. Lai, P. Bühlmann, and A. Stein, *Anal. Chem.*, 2010, **82**, 680–688.
72. A. Nann and E. Pretsch, *J. Chromatogr. A*, 1994, **676**, 437–442.
73. D. Ammann, F. Lanter, R. A. Steiner, *et al*., *Anal. Chem.*, 1981, **53**, 2267–2269.
74. M. Oehme and W. Simon, *Anal. Chim. Acta*, 1976, **86**, 21–25.
75. M. A. Messerli, I. Kurtz, and P. J. S. Smith, *Anal. Bioanal. Chem.*, 2008, **390**, 1355–1359.
76. B. R. Horrocks, M. V. Mirkin, D. T. Pierce, *et al*., *Anal. Chem.*, 1993, **65**, 1213–1224.
77. C. Wei, A. J. Bard, G. Nagy, and K. Tóth, *Anal. Chem.*, 1995, **67**, 1346–1356.
78. R. E. Gyurcsanyi, E. Pergel, R. Nagy, *et al*., *Anal. Chem.*, 2001, **73**, 2104–2111.
79. J. Szucs, E. Pretsch, and R. E. Gyurcsanyi, *Analyst*, 2009, **134**, 1601–1607.
80. J. W. Severinghaus and A. F. Bradley, *J. Appl. Physiol.*, 1958, **13**, 515.
81. W. N. Opdycke, S. J. Parks, and M. E. Meyerhoff, *Anal. Chim. Acta*, 1983, **155**, 11–20.
82. S. M. Buck, H. Xu, M. Brasuel, *et al*., *Talanta*, 2004, **63**, 41–59.
83. R. P. Buck, K. Toth, E. Gràf, *et al*., *J. Electroanal. Chem.*, 1987, **223**, 51.
84. S. Yajima, K. Tohda, P. Bühlmann, and Y. Umezawa, *Anal. Chem.*, 1997, **69**, 1919–1924.
85. A. H. J. Maas, H. F. Weisberg, R. W. Burnett, *et al*., *J. Clin. Chem. Clin. Biochem.*, 1987, **25**, 281–289.
86. O. Siggaard-Andersen, R. A. Durst, and A. H. J. Maas, *J. Clin. Chem. Clin. Biochem.*, 1987, **25**, 369–391.
87. W. Simon, D. Ammann, P. Anker, *et al*., *Ann. N. Y. Acad. Sci.*, 1984, **428**, 279–284.
88. U. Oesch, Z. Brzózka, A. Xu, and W. Simon, *Med. Biol. Eng. Comput.*, 1987, **25**, 414–419.
89. E. Bakker, A. Xu, and E. Pretsch, *Anal. Chim. Acta*, 1994, **295**, 253.
90. N. E. L. Saris, E. Mervaala, H. Karppanen, *et al*., *Clin. Chim. Acta*, 2000, **294**, 1–26.

91. E. Bakker, P. Bühlmann, and E. Pretsch, *Electroanal.*, 1999, **11**, 915–933.
92. O. Dinten, U. E. Spichiger, N. Chaniotakis, *et al.*, *Anal. Chem.*, 1991, **63**, 596–603.
93. K. Kimura, H. Tamura and T. Shono, *J. Chem. Soc., Chem. Commun.*, 1983, 492–493.
94. A. Casnati, A. Pochini, R. Ungaro, *et al.*, *Chem. Eur. J.*, 1996, **2**, 436–445.
95. H. Tamura, K. Kumami, K. Kimura, and T. Shono, *Mikrochim. Acta*, 1983, **2**, 287–296.
96. H. Yamamoto and S. Shinkai, *Chem. Lett.*, 1994, 1115–1118.
97. K. Suzuki, K. Sato, H. Hisamoto, *et al.*, *Anal. Chem.*, 1996, **68**, 208–215.
98. G. Dimeski, T. Badrick, and A. S. John, *Clin. Chim. Acta*, 2010, **411**, 309–317.
99. A. O. Okorodudu, R. W. Burnett, R. B. McComb, and G. N. Bowers, *Clin. Chem.*, 1990, **36**, 104–110.
100. E. Metzger, D. Ammann, R. Asper, and W. Simon, *Anal. Chem.*, 1986, **58**, 132–135.
101. M. Sampson, M. Ruddel, and R. J. Elin, *Clin. Chem.*, 1994, **40**, 869–872.
102. S. Faulkner, R. Kataky, D. Parker and A. Teasdale, *J. Chem. Soc., Perkin Trans. 2*, 1995, 1761–1769.
103. K. Suzuki, H. Yamada, K. Sato, *et al.*, *Anal. Chem.*, 1993, **65**, 3404–3410.
104. L. A. R. Pioda, H. A. Wachter, R. E. Dohner, and W. Simon, *Helv. Chim. Acta*, 1967, **50**, 1373–1376.
105. K. Suzuki, D. Siswanta, T. Otsuka, *et al.*, *Anal. Chem.*, 2000, **72**, 2200–2205.
106. S. Sasaki, T. Amano, G. Monma, *et al.*, *Anal. Chem.*, 2002, **74**, 4845–4848.
107. S. Y. Jon, J. Kim, M. Kim, *et al.*, *Angew. Chem. Int. Ed.*, 2001, **40**, 2116–2119.
108. S. Chandra, R. Buschbeck, and H. Lang, *Talanta*, 2006, **70**, 1087–1093.
109. W. G. McGimpsey, E. Soto, P. F. Driscoll, *et al.*, *Magn. Reson. Chem.*, 2008, **46**, 955–961.
110. G. N. Bowers, C. Brassard, and S. F. Sena, *Clin. Chem.*, 1986, **32**, 1437–1447.
111. D. Ammann, M. Güggi, E. Pretsch, and W. Simon, *Anal. Lett.*, 1975, **8**, 709–720.
112. U. Schefer, D. Ammann, E. Pretsch, *et al.*, *Anal. Chem.*, 1986, **58**, 2282–2285.
113. K. Suzuki, K. Watanabe, Y. Matsumoto, *et al.*, *Anal. Chem.*, 1995, **67**, 324–334.
114. W. Zhang, L. Jenny, and U. E. Spichiger, *Anal. Sci.*, 2000, **16**, 11–18.
115. X. J. Zhang, A. Fakler, and U. E. Spichiger, *Electroanal.*, 1998, **10**, 1174–1181.
116. R. G. Pearson, *J. Am. Chem. Soc.*, 1963, **85**, 3533–3539.
117. K. Wygladacz, A. Radu, C. Xu, *et al.*, *Anal. Chem.*, 2005, **77**, 4706–4712.
118. S. Nishizawa, P. Bühlmann, K. P. Xiao, and Y. Umezawa, *Anal. Chim. Acta*, 1998, **358**, 35–44.
119. K. P. Xiao, P. Bühlmann, S. Nishizawa, *et al.*, *Anal. Chem.*, 1997, **69**, 1038–1044.
120. H. K. Lee, H. Oh, K. C. Nam, and S. Jeon, *Sens. Actuators B*, 2005, **106**, 207–211.
121. P. Bühlmann, S. Nishizawa, K. P. Xiao, and Y. Umezawa, *Tetrahedron*, 1997, **53**, 1647–1654.
122. S. S. Koseoglu, C.-Z. Lai, C. Ferguson, and P. Bühlmann, *Electroanal.*, 2008, **20**, 331–339.
123. R. S. Hutchins, P. Molina, M. Alajarin, *et al.*, *Anal. Chem.*, 1994, **66**, 3188–3192.
124. M. Fibbioli, M. Berger, F. P. Schmidtchen, and E. Pretsch, *Anal. Chem.*, 2000, **72**, 156–160.
125. H. V. Pham, E. Pretsch, K. Fluri, *et al.*, *Helv. Chim. Acta*, 1990, **73**, 1894–1904.
126. E. Malinowska and M. E. Meyerhoff, *Anal. Chim. Acta*, 1995, **300**, 33–43.
127. Y. Kondo, T. Bührer, K. Seiler, *et al.*, *Pflügers. Arch.*, 1989, **414**, 663–668.
128. U. Schaller, E. Bakker, and E. Pretsch, *Anal. Chem.*, 1995, **67**, 3123–3132.
129. E. Steinle, S. Amemiya, P. Bühlmann, and M. Meyerhoff, *Anal. Chem.*, 2000, **72**, 5766–5773.
130. K. Wojciechowski, W. Wroblewski, and Z. Brzozka, *Pol. J. Chem.*, 2002, **76**, 671–677.
131. K. Wojciechowski, W. Wroblewski, and Z. Brzozka, *Anal. Chem.*, 2003, **75**, 3270–3273.
132. N. A. Chaniotakis, K. Jurkschat, and A. Rühlemann, *Anal. Chim. Acta*, 1993, **282**, 345–352.
133. S. Amemiya, P. Bühlmann, and K. Odashima, *Anal. Chem.*, 2003, **75**, 3329–3339.
134. L. D. Chen, D. Mandal, G. Pozzi, *et al.*, Highly selective carbonate sensors with perfluorinated matrixes. Pittsburgh Conference of Analytical Chemistry, March 2011. Atlanta, GI, USA.
135. P. C. Meier, W. E. Morf, M. Laubli, and W. Simon, *Anal. Chim. Acta*, 1984, **156**, 1–8.
136. E. Bakker, E. Pretsch, and P. Bühlmann, *Anal. Chem.*, 2000, **72**, 1127–1133.
137. M. E. Meyerhoff, E. Pretsch, D. H. Welti, and W. Simon, *Anal. Chem.*, 1987, **59**, 144.
138. H. B. Herman and G. A. Rechnitz, *Anal. Chim. Acta*, 1975, **76**, 155.
139. H. B. Herman and G. A. Rechnitz, *Science*, 1974, **184**, 1074.
140. G. A. Rechnitz, G. J. Nogle, M. R. Bellinger, and H. Lees, *Clin. Chim. Acta*, 1977, **76**, 295.
141. T. Sokalski, D. Paradowski, J. Ostaszewska, *et al.*, *Analyst*, 1996, **121**, 133–138.
142. Y. K. Hong, W. J. Yoon, H. J. Oh, *et al.*, *Electroanal.*, 1997, **9**, 865–868.
143. C. Behringer, B. Lehmann, J. P. Haug, *et al.*, *Anal. Chim. Acta*, 1990, **233**, 41.

144. M. Maj-Zurawska, T. Sokalski, J. Ostaszewska, *et al*., *Talanta*, 1997, **44**, 1641–1647.
145. S. Makarychev-Mikhailov, O. Goryacheva, J. Mortensen, *et al*., *Electroanal.*, 2003, **15**, 1291–1296.
146. Y. K. Kim, Y. H. Lee, H. Y. Lee, *et al*., *Org. Lett.*, 2003, **5**, 4003–4006.
147. H. J. Lee, I. J. Yoon, C. L. Yoo, *et al*., *Anal. Chem.*, 2000, **72**, 4694–4699.
148. K. S. Lee, J. H. Shin, S. H. Han, *et al*., *Anal. Chem.*, 1993, **65**, 3151–3155.
149. M. J. Cha, J. H. Shin, B. K. Oh, *et al*., *Anal. Chim. Acta*, 1995, **315**, 311–319.
150. D. S. Sakong, M. J. Cha, J. H. Shin, *et al*., *Sens. Actuators B*, 1996, **32**, 161–166.
151. J. Bobacka, M. Maj-Zurawska, and A. Lewenstam, *Biosens. Bioelectron.*, 2003, **18**, 245–253.
152. M. Kuratli, M. Badertscher, B. Rusterholz, and W. Simon, *Anal. Chem.*, 1993, **65**, 3473–3479.
153. G. J. Kakabadse, M. S. Al-Aziz, I. C. Hamilton, *et al*., *Analyst*, 1988, **113**, 1365–1368.
154. G. J. Kakabadse, *Sel. Electrode Rev.*, 1982, **3**, 127–187.
155. K. Odashima, P. Bühlmann, M. Sugawara, *et al*. *Advances in Supramolecular Chemistry*, ed. G. W. Gokel, JAI Press, Greenwich, CT, 1997, vol. 4, pp. 211–285.
156. E. M. G. Santos, A. N. Araugo, C. Couto, and M. Montenegro, *Electroanal.*, 2005, **17**, 1945–1951.
157. H. Hattori, M. Hoshino, T. Wakii, and A. Yuchi, *Anal. Chem.*, 2004, **76**, 5056–5062.
158. S. Sasaki, A. Hashizume, D. Citterio, *et al*., *Angew. Chem. Int. Ed.*, 2002, **41**, 3005–3007.
159. Y. Hisamatsu, K. Hasada, F. Amano, *et al*., *Chem.—Eur. J.*, 2006, **12**, 7733–7741.
160. M. H. Piao, J. Hwang, M. S. Won, *et al*., *Electroanal.*, 2008, **20**, 1293–1299.
161. E. Lindner and Y. Umezawa, *Pure Appl. Chem.*, 2008, **80**, 85–104.
162. R. Eugster, U. E. Spichiger, and W. Simon, *Anal. Chem.*, 1993, **65**, 689–695.
163. A. Ceresa and E. Pretsch, *Anal. Chim. Acta*, 1999, **395**, 41–52.
164. Y. M. Mi and E. Bakker, *Anal. Chem.*, 1999, **71**, 5279–5287.
165. M. M. Shultz, O. K. Stefanova, S. S. Mokrov, and K. N. Mikhelson, *Anal. Chem.*, 2002, **74**, 510–517.
166. Y. Kudo, T. Kobayashi, T. Ezaki, *et al*., *Anal. Sci.*, 1994, **10**, 129–131.
167. P. Ciosek and W. Wroblewski, *Analyst*, 2007, **132**, 963–978.